

# Offline-online approximation of multiscale eigenvalue problems with random defects

Dilini Kolombage\*

Barbara Verfürth\*

## Abstract

In this paper, we consider an elliptic eigenvalue problem with multiscale, randomly perturbed coefficients. For an efficient and accurate approximation of the solutions for many different realizations of the coefficient, we propose a computational multiscale method in the spirit of the Localized Orthogonal Decomposition (LOD) method together with an offline-online strategy similar to [Målqvist, Verfürth, *ESAIM Math. Model. Numer. Anal.*, 56(1):237–260, 2022]. The offline phase computes and stores local contributions to the LOD stiffness matrix for selected defect configurations. Given any perturbed coefficient, the online phase combines the pre-computed quantities in an efficient manner. We further propose a modification in the online phase, for which numerical results indicate enhanced performances for moderate and high defect probabilities. We show rigorous a priori error estimates for eigenfunctions as well as eigenvalues.

**Keywords**— eigenvalue problems, multiscale method, perturbed coefficients, offline-online strategy

**AMS subject classifications**— 65N25, 65N30, 65N12, 65N15, 35J15

## 1 Introduction

Metamaterials are modern, multiscale materials and have become increasingly popular for their unique mechanical, acoustic, or electromagnetic properties. Structurally, these materials are often constructed with a uniform distribution of very small heterogeneities, i.e., they can be represented as a periodic arrangement of unit cells. However, manufacturing mistakes that occur during the fabrication process introduce random flaws into the material structure. Therefore, the robustness study of material properties in the presence of random defects is a particularly interesting research topic in modern material sciences. From a mathematical point of view, this is modeled by an elliptic partial differential equation with a randomly perturbed coefficient. Such a stochastic partial differential equation can be solved in several ways; for instance, by stochastic Galerkin or stochastic collocation methods, see [BTZ04, DBO01, GWZ14, BNT07] for an overview. Another large class of methods consists of sampling-based approaches, in particular Monte Carlo (MC)-type methods, including multilevel and quasi MC methods. We refer to [BSZ11, CGST11, KSS12] for an overview.

In this work, we aim to obtain accurate and efficient approximations of the solutions to the stochastic PDE for many different samples. However, in a multiscale setting, standard finite element methods are, in general, not feasible due to the required fine discretization. Therefore, computational multiscale methods are employed, where we focus on the Localized Orthogonal Decomposition (LOD) method [MP21, HM14, EHMP19, MP14] in this work. The key idea is to construct problem-adapted basis functions incorporating information about the multiscale nature of the problem, so that a low-dimensional ansatz space yields sufficiently accurate solutions. However, solving the problem for many different samples remains quite expensive, as the problem-adapted basis functions must be re-computed for each realization of the (perturbed) coefficient.

The combined challenges of randomness and multiscale features have been tackled in several studies, often in the MC context and based on different multiscale methods. [Owh17] constructs so-called gamblets – hierarchical basis functions that enable sparse and orthogonal multiresolution decomposition. [ABS13] considers multilevel MC methods for problems with several, separated scales. In [BH17], the authors present a finite element-based hierarchical

---

\*Institut für Numerische Simulation, Universität Bonn, Friedrich-Hirzebruch-Allee 7, D-53115 Bonn, Germany

MC method for problems with periodic multiscale coefficients generated from an ergodic dynamical system acting on a probability space. [ZCH15] combines multiscale model reduction with data-driven approaches to obtain a reduced dimensional system in both physical and stochastic aspects. In [LBLT14], the authors propose a Multiscale Finite Element Method with a deterministic multiscale basis by taking into account the perturbative nature of the random coefficients, which have a similar structure as our model below. Very recently, [EKM24] suggests a combination of the LOD with neural networks for an efficient evaluation of the coefficient-to-basis map for general parametrized multiscale problems, that might be applicable in the random case as well. All the aforementioned works primarily consider the source problem. With regard to the eigenvalue problem, [XZO19] combines operator-adapted wavelets (gamblets) with hierarchical subspace correction to efficiently block-diagonalize the operator and refine solutions across scales. The algorithm computes eigenpairs through coarse-to-fine corrections in a multigrid fashion. [AP19] uses a preconditioned inverse iteration with an optimal multigrid solver to efficiently compute approximations of the localized low-energy eigenstates to a linear random Schrödinger operator. Note that we cannot expect such localized eigenstates in our setting.

Here, we study the elliptic eigenvalue problem with perturbed coefficients

$$-\nabla \cdot (A(x, \omega) \nabla u(x, \omega)) = \lambda(\omega) u(x, \omega) \quad \text{with} \quad A(x, \omega) = A_\varepsilon(x) + b_p(x; \omega) B_\varepsilon(x). \quad (1)$$

Detailed assumptions are postponed to the next Section 2.1. The random defects model for  $A$  is the same as in [MV22] and originally considered in [ALB11, ALB12]. Figure 1 represents two example coefficients of  $A$  generated by the background coefficient  $A_\varepsilon$  arranged in  $\varepsilon$ -sized light-green blocks, and the inclusion coefficient  $B_\varepsilon$  depicted by dark-green blocks. The random inclusion (Figure 1a) and erasure (Figure 1b) of a dark-green block represent a defect.

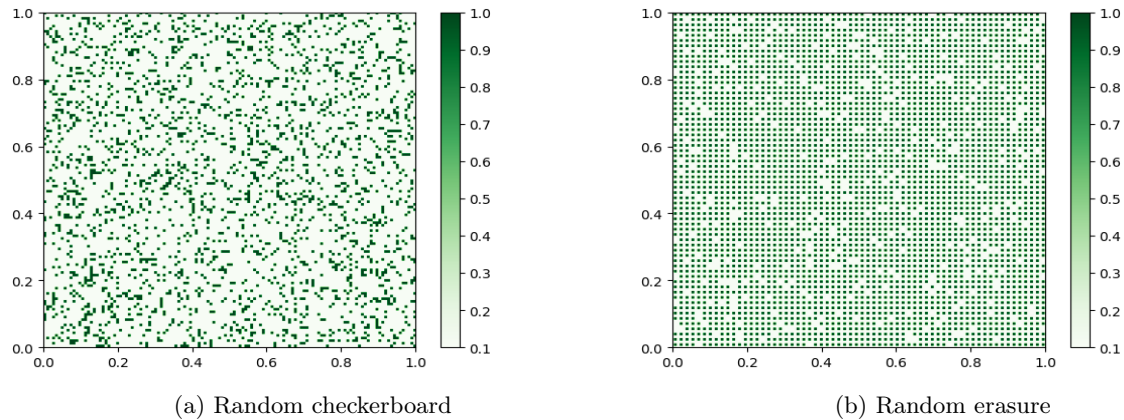


Figure 1: Weakly random coefficients with  $\varepsilon = 2^{-7}$  and  $p = 0.1$ .

Our work combines the LOD for multiscale eigenvalue problems, but without random perturbations, from [MP15] and the offline-online strategy for randomly perturbed source-type diffusion problems from [MV22]. The latter allows for a fast and efficient approximation of the LOD stiffness matrix for many realizations. To transfer the idea to eigenvalue problems, we employ the coefficient-independent finite element mass matrix for the right-hand side instead of the LOD mass matrix considered in [MP15]. Moreover, we propose a modification to the offline-online strategy improving the approximation in particular for moderate to high defect probabilities, which may be of independent interest. Besides the formulation of this method, our main contribution is a detailed a priori error analysis, based on perturbation arguments and Babuška-Osborn theory [BO91, BO89] for eigenvalue problems. As intermediate results that may be of own interest, we derive eigenfunction and eigenvalue error estimates for the Petrov-Galerkin variant of the LOD and with finite element mass matrix. We emphasize that, in contrast to [MP15], we always consider the *localized* version of the LOD method, where the corrector problems for the multiscale basis functions are computed on local patches as done in practice.

The paper is organized as follows. Section 2 introduces the model problem and recaps the offline-online strategy for the LOD method, applied to the eigenvalue problem. Further, we propose a new modification of the offline phase. In Section 3, we present our preliminary work on compact operators for eigenvalue problems that has been used as the foundation for the error analysis in Section 4. In Section 5, several numerical experiments illustrate the theoretical results and assess the performance of the proposed method. The conclusion is given in Section 6.

## 2 Setting and numerical methods

The main goal of this section is to introduce the offline-online strategy inspired by the LOD method and apply it to our eigenvalue problem. For this, we first introduce our model problem with all necessary assumptions. To derive our method, we recap the essential ingredients of the LOD. Then we discuss how to discretize the mass term on the right-hand side in the eigenvalue problem, which leads to the so-called modified LOD (MLOD). Finally, we recall the offline-online strategy – here called OLOD – based on [MV22], which allows for an efficient assembly of the left-hand side of the eigenvalue problem. We also propose an alternate variant of the OLOD at the end of the section.

### 2.1 Model problem

In this section, we describe the problem for a single sample  $\omega$ . For simplicity, we thus omit the random variable  $\omega$  in the following. Recall, however, that the final goal is to find an effective way of solving this problem for many samples. We assume the domain  $\Omega \subset \mathbb{R}^d$  to be a unit hypercube, i.e.,  $\Omega = [0, 1]^d$  with  $d \in \{1, 2, 3\}$  where we impose periodic boundary conditions. When we later discretize our problem, we always use square meshes. The weak form of the elliptic eigenvalue problem is given by: Find  $(\lambda, u) \in \mathbb{R} \times V$  such that

$$a(u, v) = \lambda m(u, v), \quad \forall v \in V, \quad (2)$$

where

$$a(u, v) := \int_{\Omega} A(x) \nabla u(x) \cdot \nabla v(x) dx, \quad m(u, v) := \int_{\Omega} u(x) v(x) dx.$$

The functional space  $V$  is the conforming finite element space given by

$$V := V_h \subseteq \mathcal{H}_{\#}^1(\Omega) = \{v_1 \in L^2(\Omega) : \nabla v_1 \in L^2(\Omega), v_1 \text{ is periodic on } \partial\Omega\},$$

where we assume the mesh size  $h$  to be small enough that we treat the solution  $u \in V_h$  as the reference solution, i.e., the error towards the exact solution in  $\mathcal{H}_{\#}^1(\Omega)$  is negligible. The energy norm and the  $L^2$ -norm are as usually defined by  $a(\cdot, \cdot) =: \|\cdot\|_{\mathcal{A}}^2 = \left\| A^{1/2} \nabla \cdot \right\|_{L^2(\Omega)}^2$  and  $m(\cdot, \cdot) =: \|\cdot\|_{L^2(\Omega)}^2$  respectively. The realization  $A \in L^\infty(\Omega, \mathbb{R})$  is a sample of a randomly perturbed coefficient which is uniformly bounded and elliptic

$$0 < \alpha \leq \operatorname{ess\,inf}_{x \in \Omega} A(x), \quad \infty > \beta \geq \operatorname{ess\,sup}_{x \in \Omega} A(x).$$

Furthermore, the underlying coefficients  $A_\varepsilon$  and  $B_\varepsilon$  of  $A(x)$  are taken to be spectrally bounded as

$$0 < \alpha \leq \operatorname{ess\,inf}_{x \in \Omega} A_{\text{per}}(x), \quad \infty > \beta \geq \operatorname{ess\,sup}_{x \in \Omega} A_{\text{per}}(x)$$

and

$$0 < \alpha \leq \operatorname{ess\,inf}_{x \in \Omega} (A_{\text{per}}(x) + B_{\text{per}}(x)), \quad \infty > \beta \geq \operatorname{ess\,sup}_{x \in \Omega} (A_{\text{per}}(x) + B_{\text{per}}(x))(x)$$

for  $A_{\text{per}}$  and  $B_{\text{per}}$  are 1-periodic with  $A_\varepsilon = A_{\text{per}}(x/\varepsilon)$  and  $B_\varepsilon = B_{\text{per}}(x/\varepsilon)$ . The multiscale parameter  $\varepsilon$  is such that  $\varepsilon = 1/n$ ,  $n \in \mathbb{N}$ ,  $n \gg 1$ . The random defects are modeled via

$$b_{p,\varepsilon}(x, \omega) = \sum_{i \in I} \chi_{\varepsilon(i+Q)}(x) \hat{b}_p^i(\omega).$$

Here, the function  $\chi$  is the characteristic function of each defect with  $Q \subseteq [0, 1]^d$  and  $I := \{\kappa \in \mathbb{Z}^d \mid \varepsilon(\kappa + Q) \subset \Omega\}$ . The independent random variables  $\hat{b}_p^i$  are independently Bernoulli distributed with probability  $p$ . Precisely,  $\hat{b}_p^i = 0$  with probability  $1 - p$  and  $\hat{b}_p^i = 1$  with probability  $p$ .

The analysis of the elliptic eigenvalue problem guarantees the existence of its eigensolutions [Eva10]. The well-posedness of the problem (2) is guaranteed by the coercivity and the continuity of the bilinear form  $a(\cdot, \cdot)$  [SF73].

For conciseness, we use the notation  $a \lesssim b$  to denote the relationship  $a \leq Cb$  where the generic constant  $C$  is independent of the discretization parameters  $H, h, k$  as well as  $\varepsilon$  throughout the rest of the paper.

## 2.2 The LOD method

The LOD method is an efficient multiscale method developed on a coarse mesh  $\mathcal{T}_H$  with a mesh size  $\varepsilon \ll H$  and a quasi-local linear operator  $I_H : V \rightarrow V_H$ ,  $I_H v = v$  for  $\forall v \in V$ . The computational finite element space  $V_H$ , with the local mesh size  $H := \max_{T \in \mathcal{T}_H} \text{diam}(T)$  is defined by

$$V_H := \mathcal{H}_{\#}^1(\Omega) \cap \mathcal{Q}_1(\mathcal{T}_H).$$

As we utilize quadrilateral meshes in this work,  $\mathcal{Q}_1(\mathcal{T}_H)$  is the space of piecewise polynomials of partial degree  $\leq 1$ . The fine space  $V_h$  on which the reference solution is defined, is constructed similarly as  $V_H$  but based on a refined mesh  $\mathcal{T}_h$ . We assume that the coarse mesh size  $H$  is an integer multiple of the periodicity length  $\varepsilon$ , which together with the periodicity of the coefficient gives additional structure to our problem. In this study, we let the bounded, surjective projection operator  $I_H$  to be constructed via

$$I_H := E_H \circ \Pi_H, \quad (3)$$

where  $\Pi_H : V \rightarrow \mathcal{Q}_1(\mathcal{T}_H)$  is the local  $L^2$ -projection and  $E_H$  is the averaging operator that maps the discontinuous functions in  $\mathcal{Q}_1(\mathcal{T}_H)$  to  $V_H$  given by

$$(E_H(v))(z) = \sum_{T \in \mathcal{T}_H, z \in \bar{T}} v|_T(z) / \text{card}\{K \in \mathcal{T}_H, z \in \bar{K}\},$$

for any  $v \in \mathcal{Q}_1(\mathcal{T}_H)$  and vertex  $z$  of  $\mathcal{T}_H$ . One more important ingredient in the LOD method is a domain localization based on element patches. For an element  $T \in \mathcal{T}_H$  and  $\mathfrak{k} \in \mathbb{N}_0$ , the patch  $U_{\mathfrak{k}}(T) \subset \Omega$  centered around  $T$  is defined by

$$\begin{aligned} U_0(T) &= T \\ U_{\mathfrak{k}+1}(T) &= \bigcup \{T \in \mathcal{T}_H : \bar{T} \cap \overline{U_{\mathfrak{k}}(T)} \neq \emptyset\}. \end{aligned}$$

The patch  $U_{\mathfrak{k}}(T)$  is called the  $\mathfrak{k}$ -th layer patch. In the LOD method, we recover the fine-scale space on these local patches by the kernel of the operator  $I_H$ , i.e.

$$W^{\mathfrak{k}} := W_H(U_{\mathfrak{k}}(T)) := \{w \in W_H : \text{supp}(w) \subseteq U_{\mathfrak{k}}(T)\},$$

where  $W_H := \ker(I_H|_V) = \{v \in V : I_H(v) = 0\} \subset V$ . Next, we define the element correction operator,  $\mathcal{C}_{\mathfrak{k},T}(A) : V \rightarrow W^{\mathfrak{k}}(T)$  that solves

$$a(\mathcal{C}_{\mathfrak{k},T}v, w) = (A\nabla(\mathcal{C}_{\mathfrak{k},T}v), \nabla w)_{U_{\mathfrak{k}}(T)} = (A\nabla v, \nabla w)_T = \int_T (A\nabla v) \cdot \nabla w dx, \quad \forall w \in W^{\mathfrak{k}}(T). \quad (4)$$

The localized correction operator  $\mathcal{C}_{\mathfrak{k}}(A) : V \rightarrow W^{\mathfrak{k}}$  is the sum

$$\mathcal{C}_{\mathfrak{k}}(A) := \sum_{T \in \mathcal{T}_H} \mathcal{C}_{\mathfrak{k},T}. \quad (5)$$

**Remark 2.1.** The ideal correction operator  $\mathcal{C} : V \rightarrow W_H$ , i.e., the correction operator taken over the whole domain, is an  $a$ -orthogonal operator satisfying

$$a((1 - \mathcal{C})v, w) = 0, \quad \text{for } v \in V \text{ and } w \in W_H.$$

The localized multiscale space is then defined by

$$V_{H,\mathfrak{k}}^{\text{ms}} := (1 - \mathcal{C}_{\mathfrak{k}}(A))V_H = \text{span}\{\varphi_z - \mathcal{C}_{\mathfrak{k}}(A)\varphi_z\}_{z \in N} \quad (6)$$

with the nodal basis  $\{\varphi_z\}_{z \in N}$  of  $V_H$ . We can now introduce the LOD method.

**The LOD method:** Find  $(\lambda_{H,\mathfrak{k}}, u_{H,\mathfrak{k}}) \in \mathbb{R} \times V_H$  such that

$$a_{\mathfrak{k}}(u_{H,\mathfrak{k}}, (1 - \mathcal{C}_{\mathfrak{k}})v) = \lambda_{H,\mathfrak{k}} m_{\mathfrak{k}}(u_{H,\mathfrak{k}}, (1 - \mathcal{C}_{\mathfrak{k}})v) \quad \forall v \in V_H \quad (7)$$

where  $a_{\mathfrak{k}}(\cdot, \cdot) = a((1 - \mathcal{C}_{\mathfrak{k}})(\cdot), (1 - \mathcal{C}_{\mathfrak{k}})(\cdot))$  and  $m_{\mathfrak{k}}(\cdot, \cdot) = m((1 - \mathcal{C}_{\mathfrak{k}})(\cdot), (1 - \mathcal{C}_{\mathfrak{k}})(\cdot))$ .

For further explanation on the LOD method, we refer to [MP14] and note the following results without proof.

**Theorem 2.2.** For any  $v \in V$  and any  $\mathfrak{k} \in \mathbb{N}_0$

$$\|(\mathcal{C} - \mathcal{C}_\mathfrak{k})v\|_{\mathcal{A}} \lesssim g(\mathfrak{k})\|v\|_{\mathcal{A}},$$

where  $g(\mathfrak{k}) = (\mathfrak{k}^{d/2} + 1) \exp\left(-c\frac{\alpha}{\beta}\mathfrak{k}\right)$ .

**Lemma 2.3.** Let  $I_H = E_H \circ \Pi_H$  be as defined in (3). Then, for  $v \in V$  and  $w \in W_H = \ker(I_H)$ ,

$$\frac{|m(v, w)_{L^2(\Omega)}|}{\|v\|_{\mathcal{A}}\|w\|_{\mathcal{A}}} \lesssim H^2.$$

Without localization, i.e.,  $\mathfrak{k} = \infty$ , the ideal LOD method for the problem (7), has been proposed and rigorously analyzed in [MP15, MP21]. Combining these estimates and proof techniques with Theorem 2.2, one arrives at the following error estimates for the eigenvalues and eigenfunctions of the LOD with localization

$$\begin{aligned} \frac{\lambda_{H,\mathfrak{k}}^l - \lambda^l}{\lambda^l} &\lesssim (g(\mathfrak{k}) + H^2)H^2 \\ \left\| u^{(l+j)} - u_{H,\mathfrak{k}}^{(l+j),\text{ms}} \right\|_{L^2(\Omega)} &\lesssim (g(\mathfrak{k}) + H^2)H \\ \left\| u^{(l+j)} - u_{H,\mathfrak{k}}^{(l+j),\text{ms}} \right\|_{\mathcal{A}} &\lesssim (\sqrt{g(\mathfrak{k})} + H)H. \end{aligned} \quad (8)$$

By choosing  $\mathfrak{k}$  large enough such that  $g(\mathfrak{k}) \sim H^2$ , we obtain the same order of convergence in (8) as in [MP21].

### 2.3 Modified LOD (MLOD) method

In the MLOD method, we consider a Petrov-Galerkin version. While the trial space is taken to be the multiscale space  $V_{H,\mathfrak{k}}^{\text{ms}}$ , the test space is considered to be the standard FE space  $V_H$ . This is advantageous in terms of computational complexity, see [EGH15] for details, and, in fact, the Petrov-Galerkin ansatz is essential for the offline-online strategy in the next section. Furthermore, we use the standard FE mass matrix instead of the LOD mass matrix. This choice is justified since the right-hand side does not involve the multiscale coefficient and thus does not need to be computed on a multiscale space. Choosing the FEM mass matrix is advantageous for our offline-online strategy as it allows to compute the right-hand side independent from the random sample. We will carefully analyze the error introduced by these modifications in Section 4.1 and 4.2.

**The MLOD method:** Find  $(\tilde{\lambda}_{H,\mathfrak{k}}, \tilde{u}_{H,\mathfrak{k}}) \in \mathbb{R} \times V_H$  such that

$$\tilde{a}_\mathfrak{k}(\tilde{u}_{H,\mathfrak{k}}, v) = \tilde{\lambda}_{H,\mathfrak{k}} \tilde{m}_\mathfrak{k}(\tilde{u}_{H,\mathfrak{k}}, v), \quad \forall v \in V_H \quad (9)$$

where  $\tilde{a}_\mathfrak{k}(\cdot, \cdot) = a((1 - \mathcal{C}_\mathfrak{k})(\cdot), (\cdot))$ , and  $\tilde{m}_\mathfrak{k}(\cdot, \cdot) = m(\cdot, \cdot)$ .

### 2.4 The offline-online strategy

The equation (6) tells us that for each realization of  $A$ , we have to re-compute the correction operator  $\mathcal{C}_\mathfrak{k}$ , and consequently the LOD basis functions. This may be computationally very demanding although the computation of  $\mathcal{C}_\mathfrak{k}$  can be parallelized. As a remedy, we use the offline-online strategy from [MV22], which we recall here to be self-contained.

Due to the Petrov-Galerkin version, for any  $v \in V_H$ , we can rewrite  $\tilde{a}_\mathfrak{k}(u_{H,\mathfrak{k}}, v)$  as a sum of element components on a patch  $U_\mathfrak{k}(T)$ , i.e.,

$$\tilde{a}_\mathfrak{k}(u_{H,\mathfrak{k}}, v) = \sum_{T \in \mathcal{T}_H} \tilde{a}_T(u_{H,\mathfrak{k}}, v_H)$$

with

$$\tilde{a}_T(u_{H,\mathfrak{k}}, v) := \int_{U_\mathfrak{k}(T)} A(x)(\chi_T \nabla u_{H,\mathfrak{k}} - \nabla(\mathcal{C}_{\mathfrak{k},T}(A)u_{H,\mathfrak{k}}))(x) \cdot \nabla v(x) dx.$$

If  $A = A_\varepsilon$ , the local contribution  $\tilde{a}_T(\cdot, \cdot)$  is exactly the same for every mesh element  $T \in \mathcal{T}_H$ . This motivates to pre-compute  $\tilde{a}_T$  for certain defect configurations, but only one single fixed  $T$ , in the offline phase and then to recombine these quantities in a suitable manner for each realization of  $A$ .

### 2.4.1 Offline phase

Fix an element  $T \in \mathcal{T}_H$  and let  $J := \{k \in \mathbb{Z}^d : \varepsilon(k+Q) \subset U_{\mathfrak{t}}(T)\}$  be the index set of possible defects in the patch  $U_{\mathfrak{t}}(T)$ . We further denote its cardinality by  $\mathcal{N} := \text{card}J$ . For the bijective mapping  $\sigma : \{1, \dots, \mathcal{N}\} \rightarrow J$ , define

$$A_i := \begin{cases} A_\varepsilon|_{U_{\mathfrak{t}}(T)}; & i = 0 \\ A_\varepsilon|_{U_{\mathfrak{t}}(T)} + \chi_{\varepsilon(\sigma(i)+Q)} B_\varepsilon; & i = 1, \dots, \mathcal{N}. \end{cases}$$

This is the offline "basis" of coefficients where  $A_i$  is constructed from  $A_\varepsilon$  by considering only a single defect. Figure 2 shows the first four offline coefficients by using such a single defect on a single patch for the random checkerboard. This is similarly done for the random erasure by removing a single element from the perfectly periodic configuration.

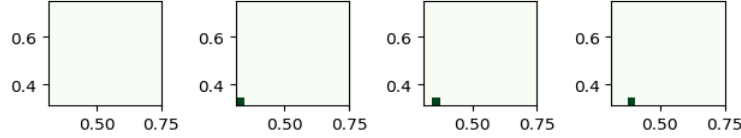


Figure 2: Offline coefficients  $A_0, A_1, A_2, A_3$  for random checkerboard

Next, we pre-compute and store the LOD stiffness matrix contributions

$$\tilde{a}_T^i(\varphi_j, \varphi_k) = \int_{U_{\mathfrak{t}}(T)} A_i(x) (\chi_T \nabla \varphi_j - \nabla (\mathcal{C}_{\mathfrak{t},T}(A_i) \varphi_j))(x) \cdot \nabla \varphi_k(x) dx.$$

for all our offline coefficients. We stress that the stiffness matrix contribution for a fixed element  $T$  is a coarse-scale object and inexpensive to store. At the same time, we can assemble the standard FE mass matrix.

### 2.4.2 Online Phase

In the online phase, the global LOD stiffness matrix that corresponds to a true coefficient  $A$  is approximated by a combination of offline quantities. Given a sample coefficient  $A$ , we locally write it as

$$A|_{U_{\mathfrak{t}}(T)} = \sum_{i=0}^{\mathcal{N}} \mu_i A_i$$

for any  $T \in \mathcal{T}_H$ . The  $\mu_i$ 's are such that  $\sum_{i=0}^{\mathcal{N}} \mu_i = 1$  for  $\mu_i \in \mathbb{R}$ ,  $i = 0, \dots, \mathcal{N}$  and each  $\mu_i$  is determined by the value of  $\hat{b}_p^j$  for some  $j$ . Furthermore,  $\mu_i \in \{0, 1\}$  for  $i = 1, \dots, \mathcal{N}$  with  $\mu_0 = 1 - \mathcal{N}_{def}$ , where  $\mathcal{N}_{def}$  denotes the number of defects on the patch  $U_{\mathfrak{t}}(T)$ . Then, we compute the offline-online LOD stiffness matrix contribution corresponding to an element  $T$  by

$$\hat{a}_{\mathfrak{t},T}(\varphi_j, \varphi_k) = \sum_{i=0}^{\mathcal{N}} \mu_i \tilde{a}_{\mathfrak{t},T}^i(\varphi_j, \varphi_k). \quad (10)$$

The global combined bilinear form  $\hat{a}$  is defined by

$$\hat{a}_{\mathfrak{t}} = \sum_{T \in \mathcal{T}_H} \hat{a}_{\mathfrak{t},T}. \quad (11)$$

The sum in (10) only contains  $\mathcal{N}_{def} + 1$  non-zero terms. Therefore, only a fraction of roughly  $p$  terms need to be considered each time. Altogether, the problem is as follows:

**The Offline-Online MLOD method (OLOD method):** Find  $(\hat{\lambda}_{H,\mathfrak{t}}, \hat{u}_{H,\mathfrak{t}}) \in \mathbb{R} \times V_H$  such that,

$$\hat{a}_{\mathfrak{t}}(\hat{u}_{H,\mathfrak{t}}, v) = \hat{\lambda}_{H,\mathfrak{t}} \hat{m}_{\mathfrak{t}}(\hat{u}_{H,\mathfrak{t}}, v), \quad \forall v \in V_H \quad (12)$$

with the mass matrix  $\widehat{m}_\mathfrak{k}(\cdot, \cdot) = \widetilde{m}_\mathfrak{k}(\cdot, \cdot) = m(\cdot, \cdot)$ . The solution  $\widehat{u}_{H,\mathfrak{k}}$  is a good  $L^2$  approximation to the exact solution  $u$ . In order to get an approximation in  $\mathcal{H}^1$ , we define the following multiscale solution, which can be efficiently computed online as well. We set

$$\widehat{u}_{H,\mathfrak{k}}^{\text{ms}} = \widehat{u}_{H,\mathfrak{k}} - \widehat{\mathcal{C}}_\mathfrak{k} \widehat{u}_{H,\mathfrak{k}} \quad \text{with} \quad \widehat{\mathcal{C}}_\mathfrak{k} := \sum_{T \in \mathcal{T}_H} \sum_{i=0}^{\mathcal{N}} \mu_i \mathcal{C}_{\mathfrak{k},T}(A_i).$$

This computation requires to store the correctors  $\mathcal{C}_{\mathfrak{k},T}(A_i)$  in the offline phase, but again only for one fixed element.

**Remark 2.4.** Computationally, the offline phase is relatively expensive, but it only needs to be computed once independent of the number of samples  $A$ . The online phase compiles a real-time stiffness matrix from the information readily available in offline storage, making it very fast.

The consistency error  $\eta_\mathfrak{k}$  defined by

$$\eta_\mathfrak{k} := \sup_{v_1 \in V_H \setminus \{0\}} \sup_{v_2 \in V_H \setminus \{0\}} \frac{|(\widetilde{a}_\mathfrak{k} - \widehat{a}_\mathfrak{k})(v_1, v_2)|}{\|v_1\|_{\mathcal{A}} \|v_2\|_{\mathcal{A}}},$$

and the error between correctors  $\mathcal{C}_\mathfrak{k}$  and  $\widehat{\mathcal{C}}_\mathfrak{k}$  are important results for the error analysis in Section 3, and have been analysed in [MV22]. There, the following upper bound on the consistency  $\widetilde{a}_\mathfrak{k} - \widehat{a}_\mathfrak{k}$ , that is computable in a posteriori manner, is established.

**Theorem 2.5.** *Define for any  $T \in \mathcal{T}_H$*

$$E_T^2 := \max_{v \in V_H : v|_T} \frac{\left\| (A^{1/2} - A^{-1/2} \overline{A}) \chi_T \nabla u - \sum_{i=0}^{\mathcal{N}} \mu_i (A^{1/2} - A^{-1/2} A_i) \nabla (\mathcal{C}_{\mathfrak{k},T}(A_i) v) \right\|_{L^2(U_\mathfrak{k}(T))}^2}{\|v\|_{\mathcal{A},T}^2}.$$

Then, for any  $v_1, v_2 \in V_H$  it holds that

$$|(\widehat{a}_\mathfrak{k} - \widetilde{a}_\mathfrak{k})(v_1, v_2)| \lesssim \mathfrak{k}^{d/2} \left( \max_{T \in \mathcal{T}_H} E_T \right) \|v_1\|_{\mathcal{A}} \|v_2\|_{\mathcal{A}}. \quad (13)$$

Furthermore, for any  $v \in V_H$ , the error between correctors is bounded by

$$\left\| (\mathcal{C}_\mathfrak{k} - \widehat{\mathcal{C}}_\mathfrak{k}) v \right\|_{\mathcal{A}}^2 \lesssim \mathfrak{k}^d \left( \max_{T \in \mathcal{T}_H} E_T \right)^2 \|v\|_{\mathcal{A}}^2. \quad (14)$$

The well-posedness of the OLOD follows due to the coercivity of  $\widehat{a}_\mathfrak{k}(v, v)$  given by

$$\widehat{a}_\mathfrak{k}(v, v) \geq (c_1 - c_2 g(\mathfrak{k}) - \eta_\mathfrak{k}) \|v\|_{\mathcal{A}}^2 \quad (15)$$

where the constants  $c_1$  and  $c_2$  only depend on the spectral bounds and the shape regularity. Clearly, there exist  $\mathfrak{k}_0 < \mathfrak{k}$  and  $\eta_0^\mathfrak{k} > \eta_\mathfrak{k}$  such that  $c_1 - c_2 g(\mathfrak{k}) - \eta_\mathfrak{k}$  is bounded below by a positive constant.

## 2.5 An alternate offline-online strategy

In this section, we define an enhanced offline-online strategy for random checkerboard-type coefficients, particularly when  $Q = [0, 1]^d$ . Note that, if  $Q$  is a proper subset of  $[0, 1]^d$ , the sum constraint  $\sum \mu_i = 1$  is necessary to guarantee the correct value of the coefficient  $A$  at points  $x$  where defects can never occur. One example is the case of random erasure and points  $x$  corresponding to the value  $A_{\text{per}}$  independent of the realization. However, in the random checkerboard case, the sum constraint  $\sum \mu_i = 1$  is merely used to guarantee uniqueness of the  $\mu_i$ . The alternate method we propose takes advantage of this by relaxing the sum constraint to be a real number  $s$  that is adapted to the underlying distribution to obtain more accurate results. In the explained random checkerboard example, we use the Bernoulli distribution. However, other probability distributions on the interval  $[\alpha, \beta]$ , such as the uniform distribution, are possible in general as well. To this end, we consider the coefficient  $A$  of the following form

$$A(x, \omega) = \sum_{j \in I} \chi_{\varepsilon(j+Q)}(x) \widetilde{\beta}_j(\omega)$$

for the alternate approach where  $\tilde{\beta}_j$  are independent and identically distributed random variables with  $\tilde{\beta}_j \in \{\alpha, \beta\}$ . The index set  $J$  and the offline coefficients  $A_i$  are defined as in Section 2.4.1. We emphasize that, for the random checkerboard case, this is just a re-writing of the coefficient.

In contrast to the sum constraint one of coefficients in the online phase defined in Section 2.4.2, we now assume  $\sum_{i=0}^{\mathcal{N}} \mu_i = s$  for some  $s \in \mathbb{R}^+$  with the property

$$A|_{U_{\mathbf{t}}(T)} = \sum_{i=0}^{\mathcal{N}} \mu_i A_i \text{ for any } T \in \mathcal{T}_H.$$

The idea of the new strategy is to find the value  $s$  using a heuristic approach to minimize the consistency error in the one-dimensional case. More precisely, as discussed in [MV22], in the one-dimensional setting with the nodal interpolation operator and patches consisting only of a single element  $T$ , the Petrov-Galerkin LOD corresponds to a finite element method with the piecewise harmonic mean as coefficient. That is

$$\tilde{a}_{\mathbf{t}}^T(u_H, v_H) = \int_T A_{\text{harm}}|_T \nabla u_H \nabla v_H dx$$

where the element-wise constant coefficient  $A_{\text{harm}}$  is given by

$$A_{\text{harm}}|_T := \left( \frac{|T|}{\varepsilon} \int_T A^{-1} dx \right)^{-1} = \frac{\varepsilon}{|T|} \frac{1}{\sum_{i=1}^{\mathcal{N}} (\tilde{\beta}_i^{-1})}.$$

We can do the same for our offline-online LOD stiffness matrix, where we denote the coefficient by  $A^\mu$ . In the following, we calculate  $A_{\text{harm}}$  and  $A_{\text{harm}}^\mu$  explicitly and then analyze their error. We obtain  $A^\mu$  as

$$A_{\text{harm}}^\mu|_T = \sum_{i=0}^{\mathcal{N}} \mu_i A_{\text{harm}}^i|_T = \mu_0 A_0 + \sum_{i=1}^{\mathcal{N}} \mu_i A_{\text{harm}}^i|_T, \quad (16)$$

where the harmonic mean of  $A_i$ ,  $A_{\text{harm}}^i$  for all  $i \geq 1$  in the case of random checkerboard can be written as

$$A_{\text{harm}}^i = \frac{\mathcal{N}}{(\mathcal{N}-1)(1/\alpha) + (1)(1/\beta)}. \quad (17)$$

The number of  $\varepsilon$  blocks in an element  $T$  denoted by  $\mathcal{N}$  is given by  $|T|/\varepsilon$ . We now need to find the correct representations of  $\mu_0$  and  $\mu_i$ ,  $i \geq 1$ . This can easily be computed from

$$\sum_{i \in J} \chi_{\varepsilon(i+Q)}(x) \tilde{\beta}_i(\omega) = \sum_{i=0}^{\mathcal{N}} \mu_i A_i = A_0 \mu_0 + \sum_{i=1}^{\mathcal{N}} \mu_i A_i,$$

for  $A_{\text{per}} = \alpha$  and  $B_{\text{per}} = \beta - \alpha$  in the random checkerboard set-up, in which the underlying linear system of equations assigns  $\tilde{\beta}_i$  value for each  $\varepsilon$  block on the patch via the characteristic function  $\chi_{\varepsilon(i+Q)}(x)$ . Hence, we deduce

$$\mu_i = \frac{\tilde{\beta}_i - \alpha s}{\beta - \alpha}, \quad j \geq 1, \quad \mu_0 = \frac{s(\beta - \alpha) - \sum_{i=1}^{\mathcal{N}} (\tilde{\beta}_i - \alpha s)}{\beta - \alpha}. \quad (18)$$

By substituting (17) and (18) into (16), we arrive at

$$\begin{aligned} A_{\text{harm}}^\mu|_T &= \frac{|T|}{\varepsilon} \frac{1}{\beta - \alpha} \left( \frac{s(\beta - \alpha) - \sum_{i=1}^{\mathcal{N}} (\tilde{\beta}_i - \alpha s)}{\mathcal{N}(1/\alpha)} + \frac{\sum_{i=1}^{\mathcal{N}} (\tilde{\beta}_i - \alpha s)}{(\mathcal{N}-1)(1/\alpha) + (1/\beta)} \right) \\ &= \frac{|T|}{\beta - \alpha} \left( \frac{s(\beta - \alpha) - \sum_{i=1}^{\mathcal{N}} (\tilde{\beta}_i - \alpha s)}{\mathcal{N}\bar{A}} + \frac{\sum_{i=1}^{\mathcal{N}} (\tilde{\beta}_i - \alpha s)}{(\mathcal{N}-1)\bar{A} + \bar{A}_s} \right) \end{aligned}$$

where  $\bar{A} = \varepsilon/\alpha$  and  $\bar{A}_s = \varepsilon/\beta$ . With this, we obtain for the error that



$$\begin{aligned}
A_{\text{harm}}|_T - A_{\text{harm}}^\mu|_T &= \frac{|T|}{\varepsilon} \left[ \frac{1}{\sum_{i=1}^{\mathcal{N}} (\tilde{\beta}_i)^{-1}} - \frac{1}{\beta - \alpha} \left( \frac{s(\beta - \alpha) - \sum_{i=1}^{\mathcal{N}} (\tilde{\beta}_i - \alpha s)}{\mathcal{N}} \alpha + \frac{\sum_{i=1}^{\mathcal{N}} (\tilde{\beta}_i - \alpha s)}{\frac{(\mathcal{N}-1)\beta + \alpha}{\alpha\beta}} \right) \right] \\
&= H(\tilde{\beta}) - s\alpha + \frac{\alpha}{\beta - \alpha} \left( \frac{\sum_{i=1}^{\mathcal{N}} (\tilde{\beta}_i - \alpha s)}{\mathcal{N}} \right) \mathcal{N} - \frac{\mathcal{N}^2 \alpha \beta}{(\beta - \alpha)} \left[ \left( \frac{\sum_{i=1}^{\mathcal{N}} (\tilde{\beta}_i - \alpha s)}{\mathcal{N}} \right) \frac{1}{(\mathcal{N}-1)\beta + \alpha} \right] \\
&= H(\tilde{\beta}) - s\alpha + \frac{M(\tilde{\beta} - \alpha s)}{(\beta - \alpha)} \frac{\alpha \mathcal{N}(\alpha - \beta)}{(\mathcal{N}-1)\beta + \alpha} \\
&= H(\tilde{\beta}) - s\alpha - \alpha M(\tilde{\beta} - \alpha s) \frac{1}{(1 - 1/\mathcal{N})\beta + \alpha/\mathcal{N}}
\end{aligned}$$

with  $H(\tilde{\beta}) = \mathcal{N} \left( \sum_{i=1}^{\mathcal{N}} (\tilde{\beta}_i)^{-1} \right)^{-1}$  and  $M(\tilde{\beta} - \alpha s) = \left( \sum_{i=1}^{\mathcal{N}} (\tilde{\beta}_i - \alpha s) \right) / \mathcal{N}$ . Our goal is to make this error as small as possible because this will imply a small consistency error. We consider the limit  $\mathcal{N} \rightarrow 0$  which corresponds to vanishing periodicity length  $\varepsilon \rightarrow 0$ , and try to find  $s$  such that the error vanishes in this limit. In other words, we find  $s$  in such a way that in the homogenization limit, there is no consistency error and our offline-online strategy retrieves the homogenized coefficient. Denote

$$L = \lim_{\mathcal{N} \rightarrow \infty} H(\tilde{\beta}) \text{ and } M = \lim_{\mathcal{N} \rightarrow \infty} M(\tilde{\beta}).$$

Note that  $L$  and  $M$  can be deduced from the probability law of  $\tilde{\beta}$  as certain expectations by the law of large numbers. Therefore, as  $\mathcal{N} \rightarrow \infty$ , we obtain

$$A_{\text{harm}}|_T - A_{\text{harm}}^\mu|_T = L - s\alpha - \frac{\alpha}{\beta} (M - \alpha s) = 0.$$

Hence the optimal  $s$  is obtained when

$$s = \frac{\beta L - \alpha M}{\alpha(\beta - \alpha)}.$$

**Example 2.6.** If  $\tilde{\beta}$  is Bernoulli distributed with probability  $p$  of having a  $\beta$  and probability  $1 - p$  for an  $\alpha$ , then we have

$$M = \alpha(1 - p) + \beta p, \quad \text{and} \quad L = \frac{\alpha\beta}{\beta + p(\alpha - \beta)}.$$

Then,  $s$  is given by

$$s = 1 + \frac{p^2(\beta - \alpha)}{\beta + p(\alpha - \beta)}.$$

Since the alternate  $s$ -value deviates from 1 more the larger  $p$  is, we expect that the influence of our new strategy is greater for larger  $p$ . This will be studied in more detail numerically in Section 5.

### 3 Preliminaries for the error analysis

Define the eigenspace spanned by orthonormal eigenfunctions  $u^{(1)}, \dots, u^{(l)}$  by the  $l$ -lowermost eigenvalues  $\lambda^{(1)}, \dots, \lambda^{(l)}$  of (2) by

$$E_l(\lambda^{(l)}) := \text{span}\{u^{(1)}, \dots, u^{(l)}\}.$$

In the following analysis, we rely on the eigenvalue analysis by using compact operators and spectral theory introduced by Babuška and Osborn in [CL02]. In the next section, we derive several preliminary results from compact operators useful in the error analysis.

Suppose  $T, T_H^1 : \mathcal{H}_\#^1(\Omega) \rightarrow \mathcal{H}_\#^1(\Omega)$  be the solution operators corresponding to the continuous eigenvalue problem written in (2) and a certain LOD based multiscale problem (say  $M1$ ) respectively, and are defined as follows.

Find  $Tf \in \mathcal{H}_\#^1$  such that

$$a(Tf, v) = m(f, v), \quad \forall v \in \mathcal{H}_\#^1. \quad (19)$$

Find  $T_H^1 f \in V_H \subset \mathcal{H}_\#^1$  such that

$$a_1(T_H^1 f, v) = m_1(f, v), \quad \forall v \in V_H. \quad (20)$$

By Babuška and Osborn theory [BO91], the eigenvalues of  $T$  are the reciprocals of the eigenvalues of the equation (2) and both problems produce the same eigenfunctions. Similarly,  $T_H^1$  has the reciprocal eigenvalues (when non-zero) and equal eigenfunctions of  $M1$ . Our error analysis of the offline-online strategy will rely on perturbation arguments, namely interpreting the offline-online LOD as variant of the LOD with different stiffness and mass matrix. Therefore, we also define an approximate solution operator  $T_H^2$  possessing the reciprocal eigenvalues and similar eigenfunctions of a second LOD based multiscale problem (say  $M2$ ) by the following.

Find  $T_H^2 f \in V_H$  such that

$$a_2(T_H^2 f, v) = m_2(f, v), \quad \forall v \in V_H. \quad (21)$$

For  $f \in V_H$ , the function  $T_H^2 f$  is defined and is taken as a map on  $V_H$ . While  $T$  is viewed as an operator on  $\mathcal{H}_\#^1$ , the operator  $T_H^1$  can be considered either to be on  $\mathcal{H}_\#^1$  or on  $V_H$ . For the perturbation analysis, we need to relate the error  $T_H^1 - T_H^2$  to the errors in  $m_1 - m_2$  and  $a_1 - a_2$  in the following.

**Lemma 3.1.** *Suppose  $T_H^1 f$  and  $T_H^2 f$  are approximated solutions to the problem (2) solved by the numerical methods as defined in problems (20) and (21) respectively. Then it holds that*

$$\begin{aligned} \left\| T_H^1 f^{(l+j)} - T_H^2 f^{(l+j)} \right\|_{\mathcal{A}}^2 &\lesssim \left| (m_1 - m_2)(f^{(l+j)}, T_H^1 f^{(l+j)} - T_H^2 f^{(l+j)}) \right| \\ &\quad + \left| (a_2 - a_1)(T_H^2 f^{(l+j)}, T_H^1 f^{(l+j)} - T_H^2 f^{(l+j)}) \right|. \end{aligned}$$

*Proof.* We deduce together with (20) and (21) that

$$\begin{aligned} \left\| T_H^1 f^{(l+j)} - T_H^2 f^{(l+j)} \right\|_{\mathcal{A}}^2 &\lesssim a_1(T_H^1 f^{(l+j)} - T_H^2 f^{(l+j)}, T_H^1 f^{(l+j)} - T_H^2 f^{(l+j)}) \\ &= a_1(T_H^1 f^{(l+j)}, T_H^1 f^{(l+j)} - T_H^2 f^{(l+j)}) - a_2(T_H^2 f^{(l+j)}, T_H^2 f^{(l+j)} - T_H^1 f^{(l+j)}) \\ &\quad + a_2(T_H^2 f^{(l+j)}, T_H^2 f^{(l+j)} - T_H^1 f^{(l+j)}) - a_1(T_H^1 f^{(l+j)}, T_H^1 f^{(l+j)} - T_H^2 f^{(l+j)}) \\ &\leq \left| (m_1 - m_2)(f^{(l+j)}, T_H^1 f^{(l+j)} - T_H^2 f^{(l+j)}) \right| \\ &\quad + \left| (a_2 - a_1)(T_H^2 f^{(l+j)}, T_H^1 f^{(l+j)} - T_H^2 f^{(l+j)}) \right|. \quad \square \end{aligned}$$

## 4 Error analysis

In this section, we derive error estimates for eigenfunctions and eigenvalues for the MLOD and the OLOD method. Recall that in the MLOD formulation, we have considered the trial space to be the multiscale space and the test space to be the classical finite element space on the coarse mesh. Consequently, the stiffness and mass matrix in the MLOD are based on the coarse FE space and different from the ones used in the Galerkin LOD method in [MP15]. We therefore start with several preliminary results particularly estimating the errors from these changes. Note that our final goal are estimates for the OLOD method, for which – similar to [BO90] – the MLOD method is introduced and analyzed as an intermediate step.

### 4.1 Preliminary estimates for the MLOD

The following two lemmas derive error estimate for choosing the FEM mass matrix and Petrov-Galerkin LOD stiffness matrix with respect to that of the LOD method.

**Lemma 4.1.** *For any  $v_1, v_2 \in V = \mathcal{H}_\#^1$ , it holds that*

$$\frac{|(m_\epsilon - \tilde{m}_\epsilon)(v_1, v_2)|}{\|v_1\|_{\mathcal{A}} \|v_2\|_{\mathcal{A}}} \lesssim H^2.$$

*Proof.* We can deduce that

$$\begin{aligned} |(m_\epsilon - \tilde{m}_\epsilon)(v_1, v_2)| &= |m(v_1 - \mathcal{C}_\epsilon v_1, v_2 - \mathcal{C}_\epsilon v_2) - m(v_1, v_2)| \\ &= |m(v_1, v_2) - m(v_1, \mathcal{C}_\epsilon v_2) - m(\mathcal{C}_\epsilon v_1, v_2) + m(\mathcal{C}_\epsilon v_1, \mathcal{C}_\epsilon v_2) - m(v_1, v_2)| \\ &\leq |m(v_1, \mathcal{C}_\epsilon v_2) + m(v_2, \mathcal{C}_\epsilon v_1)| + |m(\mathcal{C}_\epsilon v_1, \mathcal{C}_\epsilon v_2)|. \end{aligned}$$

Since  $\mathcal{C}_\mathfrak{k}(\cdot) \in W \subset V$ , by Lemma 2.3, we get that

$$\begin{aligned} |(m_\mathfrak{k} - \tilde{m}_\mathfrak{k})(v_1, v_2)| &\lesssim H^2 \left( \|v_1\|_{\mathcal{A}} \|\mathcal{C}_\mathfrak{k} v_2\|_{\mathcal{A}} + \|v_2\|_{\mathcal{A}} \|\mathcal{C}_\mathfrak{k} v_1\|_{\mathcal{A}} + \|\mathcal{C}_\mathfrak{k} v_1\|_{\mathcal{A}} \|\mathcal{C}_\mathfrak{k} v_2\|_{\mathcal{A}} \right) \\ &\leq H^2 \left[ \|v_1\|_{\mathcal{A}} \left( \|(\mathcal{C} - \mathcal{C}_\mathfrak{k})v_2\|_{\mathcal{A}} + \|\mathcal{C}v_2\|_{\mathcal{A}} \right) + \|v_2\|_{\mathcal{A}} \left( \|(\mathcal{C} - \mathcal{C}_\mathfrak{k})v_1\|_{\mathcal{A}} + \|\mathcal{C}v_1\|_{\mathcal{A}} \right) \right. \\ &\quad \left. + \left( \|(\mathcal{C} - \mathcal{C}_\mathfrak{k})v_1\|_{\mathcal{A}} + \|\mathcal{C}v_1\|_{\mathcal{A}} \right) \left( \|(\mathcal{C} - \mathcal{C}_\mathfrak{k})v_2\|_{\mathcal{A}} + \|\mathcal{C}v_2\|_{\mathcal{A}} \right) \right] \\ &\lesssim H^2 \left[ 3 + 4g(\mathfrak{k}) + g^2(\mathfrak{k}) \right] \|v_1\|_{\mathcal{A}} \|v_2\|_{\mathcal{A}}. \end{aligned}$$

The last step follows by Theorem 2.2 and the stability of  $\mathcal{C}$  in the energy norm. The notion  $g^2(\mathfrak{k})$  is used for  $(g(\mathfrak{k}))^2$ . Since  $H^2$  dominates the order, we deduce the assertion.  $\square$

**Lemma 4.2.** For any  $v_1, v_2 \in V = \mathcal{H}_\#^1$ , we have

$$\frac{|(a_\mathfrak{k} - \tilde{a}_\mathfrak{k})(v_1, v_2)|}{\|v_1\|_{\mathcal{A}} \|v_2\|_{\mathcal{A}}} \lesssim g(\mathfrak{k}).$$

*Proof.* Similar in the previous lemma, we use the definitions of  $\bar{a}(\cdot, \cdot)$  and  $\tilde{a}(\cdot, \cdot)$  to obtain

$$\begin{aligned} (a_\mathfrak{k} - \tilde{a}_\mathfrak{k})(v_1, v_2) &= a((1 - \mathcal{C}_\mathfrak{k})v_1, (1 - \mathcal{C}_\mathfrak{k})v_2) - a((1 - \mathcal{C}_\mathfrak{k})v_1, v_2) \\ &= a((1 - \mathcal{C}_\mathfrak{k})v_1, -\mathcal{C}_\mathfrak{k}v_2) \\ &= a((1 - \mathcal{C}_\mathfrak{k})v_1, (\mathcal{C} - \mathcal{C}_\mathfrak{k})v_2) - a((1 - \mathcal{C}_\mathfrak{k})v_1, \mathcal{C}v_2) \\ &= a(v_1, (\mathcal{C} - \mathcal{C}_\mathfrak{k})v_2) - a(\mathcal{C}_\mathfrak{k}v_1, (\mathcal{C} - \mathcal{C}_\mathfrak{k})v_2). \end{aligned}$$

This implies together with the stability of  $\mathcal{C}$  in the energy norm that

$$\begin{aligned} (a_\mathfrak{k} - \tilde{a}_\mathfrak{k})(v_1, v_2) &\lesssim \|v_1\|_{\mathcal{A}} \|(\mathcal{C} - \mathcal{C}_\mathfrak{k})v_2\|_{\mathcal{A}} + \|\mathcal{C}_\mathfrak{k}v_1\|_{\mathcal{A}} \|(\mathcal{C} - \mathcal{C}_\mathfrak{k})v_2\|_{\mathcal{A}} \\ &\lesssim \|(\mathcal{C} - \mathcal{C}_\mathfrak{k})v_2\|_{\mathcal{A}} \left( \|v_1\|_{\mathcal{A}} + \|(\mathcal{C} - \mathcal{C}_\mathfrak{k})v_1\|_{\mathcal{A}} + \|\mathcal{C}v_1\|_{\mathcal{A}} \right) \\ &\lesssim g(\mathfrak{k}) \left( 2 + g(\mathfrak{k}) \right) \|v_1\|_{\mathcal{A}} \|v_2\|_{\mathcal{A}}. \end{aligned}$$

Clearly,  $g(\mathfrak{k})$  decides the order of convergence.  $\square$

**Remark 4.3.** If taken  $\mathfrak{k}$  large enough such that  $g(\mathfrak{k}) = H^2$ , Lemmas 4.1 and 4.2 tells us that the error between mass matrices due to the selection of the FEM mass matrix is the same as the error due to the Petrov-Galerkin localization in the stiffness matrix.

In the next lemma, we introduce a strategy for the eigenvalue error estimates for the MLOD method.

**Lemma 4.4.** Suppose  $(\lambda, u)$  is an eigenpair of (2). Further let,  $\|v_{H,\mathfrak{k}}^{\text{ms}}\|_{L^2(\Omega)} = 1$  with  $v_{H,\mathfrak{k}}^{\text{ms}} = v_{H,\mathfrak{k}} - \mathcal{C}_\mathfrak{k}v_{H,\mathfrak{k}}$  and  $\tilde{m}_\mathfrak{k}(v_{H,\mathfrak{k}}, v_{H,\mathfrak{k}}) \neq 0$  for  $v_{H,\mathfrak{k}} \in V_H \subset \mathcal{H}_\#^1$  and  $v_{H,\mathfrak{k}}^{\text{ms}} \in V_{H,\mathfrak{k}}^{\text{ms}} \subset \mathcal{H}_\#^1$ . Consider the MLOD formulation of (2) given in (9). Then,

$$\begin{aligned} \frac{\tilde{a}_\mathfrak{k}(v_{H,\mathfrak{k}}, v_{H,\mathfrak{k}})}{\tilde{m}_\mathfrak{k}(v_{H,\mathfrak{k}}, v_{H,\mathfrak{k}})} - \lambda &\leq \|u - v_{H,\mathfrak{k}}^{\text{ms}}\|_{\mathcal{A}}^2 - \lambda \|u - v_{H,\mathfrak{k}}^{\text{ms}}\|_{L^2(\Omega)}^2 + \|(\mathcal{C} - \mathcal{C}_\mathfrak{k})v_{H,\mathfrak{k}}\|_{\mathcal{A}} \|v_{H,\mathfrak{k}}\|_{\mathcal{A}} \\ &\quad + \frac{\tilde{a}_\mathfrak{k}(v_{H,\mathfrak{k}}, v_{H,\mathfrak{k}})}{\tilde{m}_\mathfrak{k}(v_{H,\mathfrak{k}}, v_{H,\mathfrak{k}})} \left( m_\mathfrak{k}(v_{H,\mathfrak{k}}, v_{H,\mathfrak{k}}) - \tilde{m}_\mathfrak{k}(v_{H,\mathfrak{k}}, v_{H,\mathfrak{k}}) \right). \end{aligned}$$

*Proof.* Observe that

$$\|u - v_{H,\mathfrak{k}}^{\text{ms}}\|_{\mathcal{A}}^2 - \lambda \|u - v_{H,\mathfrak{k}}^{\text{ms}}\|_{L^2(\Omega)}^2 = \|u\|_{\mathcal{A}}^2 - 2a(u, v_{H,\mathfrak{k}}^{\text{ms}}) + \|v_{H,\mathfrak{k}}^{\text{ms}}\|_{\mathcal{A}}^2 - \lambda \|u\|_{L^2(\Omega)}^2 + 2\lambda m(u, v_{H,\mathfrak{k}}^{\text{ms}}) - \lambda \|v_{H,\mathfrak{k}}^{\text{ms}}\|_{L^2(\Omega)}^2. \quad (22)$$

Since  $a(u, v_{H,\mathfrak{k}}^{\text{ms}}) = \lambda m(u, v_{H,\mathfrak{k}}^{\text{ms}})$  holds by (2) and we have that  $\|u\|_{\mathcal{A}}^2 = a(u, u) = \lambda m(u, u) = \lambda \|u\|_{L^2(\Omega)}^2$ , we get by the normalization  $\|v_{H,\mathfrak{k}}^{\text{ms}}\|_{L^2(\Omega)} = 1$ , and (22) that

$$\|u - v_{H,\mathfrak{k}}^{\text{ms}}\|_{\mathcal{A}}^2 - \lambda \|u - v_{H,\mathfrak{k}}^{\text{ms}}\|_{L^2(\Omega)}^2 = a(v_{H,\mathfrak{k}}^{\text{ms}}, v_{H,\mathfrak{k}}^{\text{ms}}) - \lambda. \quad (23)$$

Recall that  $\tilde{a}_\mathfrak{k}(\cdot, \cdot) = a((\cdot)_\mathfrak{k}^{\text{ms}}, (\cdot))$  and  $\tilde{m}_\mathfrak{k}(\cdot, \cdot) = m((\cdot), (\cdot)) = \|(\cdot)\|_{L^2(\Omega)}^2$ . Then we deduce that

$$\begin{aligned} a(v_{H,\mathfrak{k}}^{\text{ms}}, v_{H,\mathfrak{k}}^{\text{ms}}) &= a(v_{H,\mathfrak{k}}^{\text{ms}}, (1 - \mathcal{C}_\mathfrak{k})v_{H,\mathfrak{k}}) \\ &= a(v_{H,\mathfrak{k}}^{\text{ms}}, v_{H,\mathfrak{k}}) - a((1 - \mathcal{C}_\mathfrak{k})v_{H,\mathfrak{k}}, \mathcal{C}_\mathfrak{k}v_{H,\mathfrak{k}}) \\ &= a(v_{H,\mathfrak{k}}^{\text{ms}}, v_{H,\mathfrak{k}}) - a(v_{H,\mathfrak{k}} - \mathcal{C}v_{H,\mathfrak{k}}, \mathcal{C}_\mathfrak{k}v_{H,\mathfrak{k}}) - a((\mathcal{C} - \mathcal{C}_\mathfrak{k})v_{H,\mathfrak{k}}, \mathcal{C}_\mathfrak{k}v_{H,\mathfrak{k}}). \end{aligned}$$

Due to the  $a$ -orthogonality, and the stability of  $\mathcal{C}_\mathfrak{k}$  in the energy norm we derive

$$\begin{aligned} a(v_{H,\mathfrak{k}}^{\text{ms}}, v_{H,\mathfrak{k}}) &= a(v_{H,\mathfrak{k}}^{\text{ms}}, v_{H,\mathfrak{k}}^{\text{ms}}) + a((\mathcal{C} - \mathcal{C}_\mathfrak{k})v_{H,\mathfrak{k}}, \mathcal{C}_\mathfrak{k}v_{H,\mathfrak{k}}) \\ &\leq a(v_{H,\mathfrak{k}}^{\text{ms}}, v_{H,\mathfrak{k}}^{\text{ms}}) + \|(\mathcal{C} - \mathcal{C}_\mathfrak{k})v_{H,\mathfrak{k}}\|_{\mathcal{A}} \|v_{H,\mathfrak{k}}\|_{\mathcal{A}}. \end{aligned} \quad (24)$$

Together with (23), we arrive at

$$[a(v_{H,\mathfrak{k}}^{\text{ms}}, v_{H,\mathfrak{k}}) - \lambda] \leq \|u - v_{H,\mathfrak{k}}^{\text{ms}}\|_{\mathcal{A}}^2 - \lambda \|u - v_{H,\mathfrak{k}}^{\text{ms}}\|_{L^2(\Omega)}^2 + \|(\mathcal{C} - \mathcal{C}_\mathfrak{k})v_{H,\mathfrak{k}}\|_{\mathcal{A}} \|v_{H,\mathfrak{k}}\|_{\mathcal{A}}.$$

Using this inequality and our definitions, we obtain that

$$\begin{aligned} \frac{\tilde{a}_\mathfrak{k}(v_{H,\mathfrak{k}}, v_{H,\mathfrak{k}})}{\tilde{m}_\mathfrak{k}(v_{H,\mathfrak{k}}, v_{H,\mathfrak{k}})} - \lambda &= [\tilde{a}_\mathfrak{k}(v_{H,\mathfrak{k}}, v_{H,\mathfrak{k}}) - \lambda] + \left[ \frac{\tilde{a}_\mathfrak{k}(v_{H,\mathfrak{k}}, v_{H,\mathfrak{k}})}{\tilde{m}_\mathfrak{k}(v_{H,\mathfrak{k}}, v_{H,\mathfrak{k}})} - \tilde{a}_\mathfrak{k}(v_{H,\mathfrak{k}}, v_{H,\mathfrak{k}}) \right] \\ &= [\tilde{a}_\mathfrak{k}(v_{H,\mathfrak{k}}, v_{H,\mathfrak{k}}) - \lambda] + \left[ \frac{\tilde{a}_\mathfrak{k}(v_{H,\mathfrak{k}}, v_{H,\mathfrak{k}})}{\tilde{m}_\mathfrak{k}(v_{H,\mathfrak{k}}, v_{H,\mathfrak{k}})} \|v_{H,\mathfrak{k}}^{\text{ms}}\|_{L^2(\Omega)}^2 - \frac{\tilde{a}_\mathfrak{k}(v_{H,\mathfrak{k}}, v_{H,\mathfrak{k}})}{\tilde{m}_\mathfrak{k}(v_{H,\mathfrak{k}}, v_{H,\mathfrak{k}})} \tilde{m}_\mathfrak{k}(v_{H,\mathfrak{k}}, v_{H,\mathfrak{k}}) \right] \\ &= [\tilde{a}_\mathfrak{k}(v_{H,\mathfrak{k}}, v_{H,\mathfrak{k}}) - \lambda] + \frac{\tilde{a}_\mathfrak{k}(v_{H,\mathfrak{k}}, v_{H,\mathfrak{k}})}{\tilde{m}_\mathfrak{k}(v_{H,\mathfrak{k}}, v_{H,\mathfrak{k}})} [m_\mathfrak{k}(v_{H,\mathfrak{k}}, v_{H,\mathfrak{k}}) - \tilde{m}_\mathfrak{k}(v_{H,\mathfrak{k}}, v_{H,\mathfrak{k}})] \\ &= a(v_{H,\mathfrak{k}}^{\text{ms}}, v_{H,\mathfrak{k}}) - \lambda + \frac{\tilde{a}_\mathfrak{k}(v_{H,\mathfrak{k}}, v_{H,\mathfrak{k}})}{\tilde{m}_\mathfrak{k}(v_{H,\mathfrak{k}}, v_{H,\mathfrak{k}})} [m_\mathfrak{k}(v_{H,\mathfrak{k}}, v_{H,\mathfrak{k}}) - \tilde{m}_\mathfrak{k}(v_{H,\mathfrak{k}}, v_{H,\mathfrak{k}})] \\ &\leq \|u - v_{H,\mathfrak{k}}^{\text{ms}}\|_{\mathcal{A}}^2 - \lambda \|u - v_{H,\mathfrak{k}}^{\text{ms}}\|_{L^2(\Omega)}^2 + \|(\mathcal{C} - \mathcal{C}_\mathfrak{k})v_{H,\mathfrak{k}}\|_{\mathcal{A}} \|v_{H,\mathfrak{k}}\|_{\mathcal{A}} \\ &\quad + \frac{\tilde{a}_\mathfrak{k}(v_{H,\mathfrak{k}}, v_{H,\mathfrak{k}})}{\tilde{m}_\mathfrak{k}(v_{H,\mathfrak{k}}, v_{H,\mathfrak{k}})} [m_\mathfrak{k}(v_{H,\mathfrak{k}}, v_{H,\mathfrak{k}}) - \tilde{m}_\mathfrak{k}(v_{H,\mathfrak{k}}, v_{H,\mathfrak{k}})]. \quad \square \end{aligned}$$

## 4.2 Main results for the MLOD method

In this section, we present the main estimates for MLOD eigenfunctions and eigenvalues.

**Theorem 4.5** (Eigenfunction estimates). *Let  $\lambda^{(l)}$  be an eigenvalue of multiplicity  $r$ , i.e.,  $\lambda^{(l)} = \dots = \lambda^{(l+r-1)}$  with the corresponding eigenspace  $E_{l+j}$ ,  $j = 0, 1, \dots, r-1$  spanned by the  $r$ -many orthonormal basis functions with  $\|u^{(l+j)}\|_{\mathcal{H}^1} = 1$ . Suppose the pairs  $(\lambda_{H,\mathfrak{k}}^{(l)}, u_{H,\mathfrak{k}}^{(l),\text{ms}}), \dots, (\lambda_{H,\mathfrak{k}}^{(l+r-1)}, u_{H,\mathfrak{k}}^{(l+r-1),\text{ms}})$  approximate the LOD problem in (7) with  $\|u_{H,\mathfrak{k}}^{(l+j),\text{ms}}\|_{L^2(\Omega)} = 1$  and the pairs  $(\tilde{\lambda}_{H,\mathfrak{k}}^{(l)}, \tilde{u}_{H,\mathfrak{k}}^{(l),\text{ms}}), \dots, (\tilde{\lambda}_{H,\mathfrak{k}}^{(l+r-1)}, \tilde{u}_{H,\mathfrak{k}}^{(l+r-1),\text{ms}})$  approximate the problem in (9) with  $\|\tilde{u}_{H,\mathfrak{k}}^{(l+j),\text{ms}}\|_{L^2(\Omega)} = 1 \forall j$ . Further assume  $\overline{E}_{l+j}^\mathfrak{k}$  and  $\tilde{E}_{l+j}^\mathfrak{k}$  to be the eigenspace spanned by the  $r$ -many basis functions corresponding to  $\lambda_{H,\mathfrak{k}}^{(l+j)}$  and  $\tilde{\lambda}_{H,\mathfrak{k}}^{(l+j)}$ ,  $\forall j$  respectively. If  $l+r-1 \leq N$ , then, there exists a function  $u^{(l+j)} \in E_{l+j}$  such that, for all  $j = 0, 1, \dots, r-1$ ,*

$$\|u^{(l+j)} - \tilde{u}_{H,\mathfrak{k}}^{(l+j),\text{ms}}\|_{\mathcal{A}} \lesssim H^2 + g(\mathfrak{k}).$$

We emphasize that approximation order  $H^2$  is the same as for the Galerkin LOD method (with or without localization) presented in [MP15], cf. (8). Note that the localization parameter  $\mathfrak{k}$  can be chosen sufficiently large to obtain an overall convergence order  $H^2$ .

*Proof.* For any  $j = 0, 1, \dots, r-1$ , with  $u^{(l+j)} \in E_{l+j}$  we have that

$$\begin{aligned} \|u^{(l+j)} - \tilde{u}_{H,\mathfrak{k}}^{(l+j),\text{ms}}\|_{\mathcal{A}} &\leq \|u^{(l+j)} - u_{H,\mathfrak{k}}^{(l+j),\text{ms}}\|_{\mathcal{A}} + \|u_{H,\mathfrak{k}}^{(l+j),\text{ms}} - \tilde{u}_{H,\mathfrak{k}}^{(l+j),\text{ms}}\|_{\mathcal{A}} \\ &\leq \|u^{(l+j)} - u_{H,\mathfrak{k}}^{(l+j),\text{ms}}\|_{\mathcal{A}} + \|u_{H,\mathfrak{k}}^{(l+j)} - \tilde{u}_{H,\mathfrak{k}}^{(l+j)}\|_{\mathcal{A}} + \|\mathcal{C}_\mathfrak{k}(u_{H,\mathfrak{k}}^{(l+j)} - \tilde{u}_{H,\mathfrak{k}}^{(l+j)})\|_{\mathcal{A}} \\ &\leq \|u^{(l+j)} - u_{H,\mathfrak{k}}^{(l+j),\text{ms}}\|_{\mathcal{A}} + 2\|u_{H,\mathfrak{k}}^{(l+j)} - \tilde{u}_{H,\mathfrak{k}}^{(l+j)}\|_{\mathcal{A}} + \|(\mathcal{C} - \mathcal{C}_\mathfrak{k})(\overline{u}_{H,\mathfrak{k}}^{(l+j)} - \tilde{u}_{H,\mathfrak{k}}^{(l+j)})\|_{\mathcal{A}} \\ &\lesssim H^2 + (g(\mathfrak{k}))^{1/2} H + (2 + g(\mathfrak{k})) \|u_{H,\mathfrak{k}}^{(l+j)} - \tilde{u}_{H,\mathfrak{k}}^{(l+j)}\|_{\mathcal{A}} \end{aligned}$$

where the second last step follows from the stability of  $\mathcal{C}$  in the energy norm. The last step is due to (8) and Theorem 2.2. The second term can be estimated using the compact operators. Suppose in Lemma 3.1,  $M1$  is given by the LOD solving (7) and  $M2$  is given by the MLOD solving (9). Then, with  $a_1 = a_\mathfrak{k}$ ,  $a_2 = \tilde{a}_\mathfrak{k}$ ,  $m_1 = m_\mathfrak{k}$ ,  $m_2 = \tilde{m}_\mathfrak{k}$ ,  $T_H^1 = T_H^\mathfrak{k}$  and  $T_H^2 = \tilde{T}_H^\mathfrak{k}$ , it yields

$$\begin{aligned} \left\| T_H^\mathfrak{k} f^{(l+j)} - \tilde{T}_H^\mathfrak{k} f^{(l+j)} \right\|_{\mathcal{A}}^2 &\lesssim (m_\mathfrak{k} - \tilde{m}_\mathfrak{k}) (f^{(l+j)}, T_H^\mathfrak{k} f^{(l+j)} - \tilde{T}_H^\mathfrak{k} f^{(l+j)}) \\ &\quad + (\tilde{a}_\mathfrak{k} - a_\mathfrak{k}) (\tilde{T}_H^\mathfrak{k} f^{(l+j)}, T_H^\mathfrak{k} f^{(l+j)} - \tilde{T}_H^\mathfrak{k} f^{(l+j)}). \end{aligned}$$

Since  $\tilde{T}_H^\mathfrak{k} f^{(l+j)}$  solves for (7), by Lemma 4.1 and Lemma 4.2, we obtain that

$$\left\| T_H^\mathfrak{k} f^{(l+j)} - \tilde{T}_H^\mathfrak{k} f^{(l+j)} \right\|_{\mathcal{A}} \lesssim \|f\|_{\mathcal{A}} H^2 + \left\| \tilde{T}_H^\mathfrak{k} f^{(l+j)} \right\|_{\mathcal{A}} g(\mathfrak{k}).$$

Since  $T_H^\mathfrak{k} f^{(l+j)}, \tilde{T}_H^\mathfrak{k} f^{(l+j)} \in V_H$ , there exist some  $v_0, \tilde{v}_0 \in V_H$  such that  $T_H^\mathfrak{k} f^{(l+j)} = v_0$  and  $\tilde{T}_H^\mathfrak{k} f^{(l+j)} = \tilde{v}_0$  solving (20) and (21) for LOD and MLOD respectively. On the other hand, (7) and (9) solve for eigensolutions on  $V_H$  for the LOD and MLOD respectively. Moreover, the pair (20) and (7) (similarly (21) and (9)) produce the same eigenfunctions and reciprocal eigenvalues to the LOD and MLOD problems. Therefore, for  $f \in E_{(l+j)}$  with  $\left\| f^{(l+j)} \right\|_{\mathcal{H}^1(\Omega)} = 1$ , by the analysis of [BO90] we obtain that

$$\left\| u_{H,\mathfrak{k}}^{(l+j)} - \tilde{u}_{H,\mathfrak{k}}^{(l+j)} \right\|_{\mathcal{A}} \lesssim H^2 + g(\mathfrak{k}) \left\| \tilde{u}_{H,\mathfrak{k}}^{(l+j)} \right\|_{\mathcal{A}}. \quad (25)$$

We are left to bound  $\left\| \tilde{u}_{H,\mathfrak{k}}^{(l+j)} \right\|_{\mathcal{A}}$ . For  $\mathfrak{k}$  large enough, by the coercivity of  $\tilde{a}(\cdot, \cdot)$  [EGH15], for any  $v \in \mathcal{H}_\#^1$

$$\|v\|_{\mathcal{A}}^2 \lesssim \tilde{a}_\mathfrak{k}(v, v).$$

If we set  $v = \tilde{u}_{H,\mathfrak{k}}^{(l+j)}$ , we get that

$$\left\| \tilde{u}_{H,\mathfrak{k}}^{(l+j)} \right\|_{\mathcal{A}}^2 \leq \left| \tilde{a}_\mathfrak{k}(\tilde{u}_{H,\mathfrak{k}}^{(l+j)}, \tilde{u}_{H,\mathfrak{k}}^{(l+j)}) \right| = \left| \tilde{\lambda}_{H,\mathfrak{k}}^l \tilde{m}_\mathfrak{k}(\tilde{u}_{H,\mathfrak{k}}^{(l+j)}, \tilde{u}_{H,\mathfrak{k}}^{(l+j)}) \right| \leq \tilde{C}_\lambda \left| \lambda^{(l)} \right| \left| m(\tilde{u}_{H,\mathfrak{k}}^{(l+j)}, \tilde{u}_{H,\mathfrak{k}}^{(l+j)}) \right| = \tilde{C}_\lambda \left| \lambda^{(l)} \right| \left\| \tilde{u}_{H,\mathfrak{k}}^{(l+j)} \right\|_{L^2(\Omega)}^2. \quad (26)$$

The third step follows due to  $\left| \tilde{\lambda}_{H,\mathfrak{k}}^{(l)} \right| \leq c \left| \lambda^{(l)} \right|$ , for some  $c \in \mathbb{R}$  by Babuška-Osborn theory because Lemma 3.1 and the known analysis of the source problem (see above) in particular yield convergence of  $\tilde{\lambda}_{H,\mathfrak{k}}^{(l)}$  to  $\lambda^{(l)}$  for  $H \rightarrow 0$  and  $\mathfrak{k} \rightarrow \infty$ . Since  $\left\| \tilde{u}_{H,\mathfrak{k}}^{(l+j)} \right\|_{L^2(\Omega)} = \left\| I_H \tilde{u}_{H,\mathfrak{k}}^{(l+j),ms} \right\|_{L^2(\Omega)} \leq \tilde{C}_\mathfrak{k} \left\| \tilde{u}_{H,\mathfrak{k}}^{(l+j),ms} \right\|_{L^2(\Omega)} = \tilde{C}_\mathfrak{k}$  by definition,  $\left\| \tilde{u}_{H,\mathfrak{k}}^{(l+j)} \right\|_{\mathcal{A}}$  is clearly bounded above by a positive constant. Therefore, it holds that

$$\left\| u^{(l+j)} - \tilde{u}_{H,\mathfrak{k}}^{(l+j),ms} \right\|_{\mathcal{A}} \lesssim 2H^2 + 2g(\mathfrak{k}) + H^2 g(\mathfrak{k}) + g^2(\mathfrak{k}) + \left( g(\mathfrak{k}) \right)^{1/2} H + H^2.$$

The result easily follows by only considering the dominating terms.  $\square$

We now turn to the eigenvalue estimate. Typically, one expects the square of the eigenfunction error, but here the perturbation terms need to be considered as well. Consequently, we obtain a convergence order of  $H^2$  also for the eigenvalues and stress that this reduced order in comparison to [MP15] stems from the use of the FE mass matrix, cf. Lemma 4.1.

**Theorem 4.6** (Eigenvalue estimates). *Suppose  $\lambda^{(l)}$  and  $\tilde{\lambda}_{H,\mathfrak{k}}^{(l)}$  are the  $l$ -th eigenvalues of (2) and (9) respectively with a multiplicity  $r$ . If  $\left\| \tilde{u}_{H,\mathfrak{k}}^{(l+j),ms} \right\|_{L^2(\Omega)} = 1$  for each  $j = 0, \dots, r-1$ , then,*

$$\left| \frac{\tilde{\lambda}_{H,\mathfrak{k}}^{(l)} - \lambda^{(l)}}{\lambda^{(l)}} \right| \lesssim g(\mathfrak{k}) + H^2.$$

*Proof.* Note that  $\frac{\tilde{a}_\mathfrak{k}(\tilde{u}_{H,\mathfrak{k}}^{(l)}, \tilde{u}_{H,\mathfrak{k}}^{(l)})}{\tilde{m}_\mathfrak{k}(\tilde{u}_{H,\mathfrak{k}}^{(l)}, \tilde{u}_{H,\mathfrak{k}}^{(l)})} = \tilde{\lambda}_{H,\mathfrak{k}}^{(l)}$ . Also remind that  $\lambda^{(l)}$  of (2) is positive. We use Lemma 4.4 with  $v_{H,\mathfrak{k}} = \tilde{u}_{H,\mathfrak{k}}^{(l+j)}$  and Lemma 4.1 to obtain that

$$\begin{aligned} \tilde{\lambda}_{H,\mathfrak{k}}^{(l)} - \lambda^{(l)} &= \frac{\tilde{a}_\mathfrak{k}(\tilde{u}_{H,\mathfrak{k}}^{(l+j)}, \tilde{u}_{H,\mathfrak{k}}^{(l+j)})}{\tilde{m}_\mathfrak{k}(\tilde{u}_{H,\mathfrak{k}}^{(l+j)}, \tilde{u}_{H,\mathfrak{k}}^{(l+j)})} - \lambda^{(l)} \\ &\leq \left\| u^{(l+j)} - \tilde{u}_{H,\mathfrak{k}}^{(l+j),\text{ms}} \right\|_{\mathcal{A}}^2 - \lambda^l \left\| u^{(l+j)} - \tilde{u}_{H,\mathfrak{k}}^{(l+j),\text{ms}} \right\|_{L^2(\Omega)}^2 + \left\| (\mathfrak{C} - \mathfrak{C}_\mathfrak{k}) \tilde{u}_{H,\mathfrak{k}}^{(l+j)} \right\|_{\mathcal{A}} \left\| \tilde{u}_{H,\mathfrak{k}}^{(l+j)} \right\|_{\mathcal{A}} \\ &\quad + \tilde{\lambda}_{H,\mathfrak{k}}^l \left( m_\mathfrak{k}(\tilde{u}_{H,\mathfrak{k}}^{(l+j)}, \tilde{u}_{H,\mathfrak{k}}^{(l+j)}) - \tilde{m}_\mathfrak{k}(\tilde{u}_{H,\mathfrak{k}}^{(l+j)}, \tilde{u}_{H,\mathfrak{k}}^{(l+j)}) \right). \end{aligned}$$

Since  $\left| \tilde{\lambda}_{H,\mathfrak{k}}^{(l)} \right|$  can be bounded above by the absolute continuous eigenvalue, by Theorem 4.5, Theorem 2.2 and Lemma 4.1, we derive that

$$\left| \frac{\tilde{\lambda}_{H,\mathfrak{k}}^{(l)} - \lambda^{(l)}}{\lambda^{(l)}} \right| \lesssim \left( H^2 + g(\mathfrak{k}) \right)^2 + g(\mathfrak{k}) \left\| \tilde{u}_{H,\mathfrak{k}}^{(l+j)} \right\|_{\mathcal{A}}^2 + H^2. \quad (27)$$

The assertion follows since  $\left\| \tilde{u}_{H,\mathfrak{k}}^{(l+j)} \right\|_{\mathcal{A}}^2$  can be bounded above as previously shown.  $\square$

**Remark 4.7.** Given that  $g(\mathfrak{k}) \approx H^2$ , if we compare equation (27) with the eigenvalue results form (7), we can clearly see that the reduction of order from  $H^4$  to  $H^2$  follows as a consequence of the localization error regardless of the choice of the mass matrix as long as the latter maintains a convergence rate  $H^2$ . Therefore, by choosing the FEM mass matrix instead of a LOD based mass matrix, we obtain an efficient solver at the same convergence rate  $H^2$ .

### 4.3 OLOD method

We now present our analytical results for the eigenfunctions and eigenvalues in the OLOD method. As explained in earlier sections, we utilize the MLOD results as an intermediate step between the continuous and OLOD solutions. Recall that moving from the MLOD to the OLOD method, only the stiffness matrix on the left-hand side changes. Analyzing this additional consistency error with the techniques already used for the MLOD method, we show the same error rates now also for the OLOD method.

**Theorem 4.8** (Eigenfunction estimates). *Suppose the OLOD problem in (12) is well-posed. Let  $\lambda^{(l)}$  be an eigenvalue of (2) of multiplicity  $r$  with the corresponding eigenspace  $E_{l+j}$ ,  $j = 0, 1, \dots, r-1$  spanned by the  $r$ -many orthonormal basis functions. Further let  $(\lambda^{(l)}, u^{(l+j)})$  and  $(\tilde{\lambda}_{H,\mathfrak{k}}^{(l)}, \hat{u}_{H,\mathfrak{k}}^{(l+j),\text{ms}})$  be the  $l$ -th solution to (2) and the  $l$ -th approximated solution to (12) respectively where  $\hat{u}_{H,\mathfrak{k}}^{(l+j),\text{ms}} = \hat{u}_{H,\mathfrak{k}}^{(l+j)} - \widehat{\mathfrak{C}}_\mathfrak{k} \hat{u}_{H,\mathfrak{k}}^{(l+j)}$ ,  $\hat{u}_{H,\mathfrak{k}}^{(l+j)} \in V_H$ . For any  $j$ , assume the normalization condition  $\left\| \hat{u}_{H,\mathfrak{k}}^{(l+j),\text{ms}} \right\|_{L^2(\Omega)} = 1$ . Denote  $\widehat{E}_{l+j}^\mathfrak{k}$  to be the eigenspace spanned by the  $r$ -many approximated basis functions of (12). If  $l+r-1 \leq N$ , there exists a function  $u_H^{(l+j),\text{ms}} \in E_{l+j}$  such that for all  $j$  the following holds:*

$$\left\| u^{(l+j)} - \hat{u}_{H,\mathfrak{k}}^{(l+j),\text{ms}} \right\|_{\mathcal{A}} \lesssim H^2 + g(\mathfrak{k}) + \left( \max_{T \in \mathcal{T}_H} E_T \right) \mathfrak{k}^{d/2}.$$

*Proof.* For  $j = 0, 1, \dots, r-1$ , we have that

$$\begin{aligned} \left\| u^{(l+j)} - \hat{u}_{H,\mathfrak{k}}^{(l+j),\text{ms}} \right\|_{\mathcal{A}} &\leq \left\| u^{(l+j)} - \tilde{u}_{H,\mathfrak{k}}^{(l+j),\text{ms}} \right\|_{\mathcal{A}} + \left\| \tilde{u}_{H,\mathfrak{k}}^{(l+j)} - \mathfrak{C}_\mathfrak{k} \tilde{u}_{H,\mathfrak{k}}^{(l+j)} - \hat{u}_{H,\mathfrak{k}}^{(l+j)} + \widehat{\mathfrak{C}}_\mathfrak{k} \hat{u}_{H,\mathfrak{k}}^{(l+j)} \right\|_{\mathcal{A}} \\ &\quad + \left\| \widehat{\mathfrak{C}}_\mathfrak{k} \hat{u}_{H,\mathfrak{k}}^{(l+j)} + \mathfrak{C}_\mathfrak{k} \hat{u}_{H,\mathfrak{k}}^{(l+j)} - \mathfrak{C}_\mathfrak{k} \hat{u}_{H,\mathfrak{k}}^{(l+j)} - \mathfrak{C}_\mathfrak{k} \tilde{u}_{H,\mathfrak{k}}^{(l+j)} \right\|_{\mathcal{A}} \\ &\leq \left\| u^{(l+j)} - \tilde{u}_{H,\mathfrak{k}}^{(l+j),\text{ms}} \right\|_{\mathcal{A}} + \left\| \tilde{u}_{H,\mathfrak{k}}^{(l+j)} - \hat{u}_{H,\mathfrak{k}}^{(l+j)} \right\|_{\mathcal{A}} \\ &\quad + \left\| \mathfrak{C}_\mathfrak{k} (\tilde{u}_{H,\mathfrak{k}}^{(l+j)} - \hat{u}_{H,\mathfrak{k}}^{(l+j)}) \right\|_{\mathcal{A}} + \left\| (\widehat{\mathfrak{C}}_\mathfrak{k} - \mathfrak{C}_\mathfrak{k}) \hat{u}_{H,\mathfrak{k}}^{(l+j)} \right\|_{\mathcal{A}} \\ &\lesssim \left\| u^{(l+j)} - \tilde{u}_{H,\mathfrak{k}}^{(l+j),\text{ms}} \right\|_{\mathcal{A}} + 2 \left\| \tilde{u}_{H,\mathfrak{k}}^{(l+j)} - \hat{u}_{H,\mathfrak{k}}^{(l+j)} \right\|_{\mathcal{A}} + \left\| (\widehat{\mathfrak{C}}_\mathfrak{k} - \mathfrak{C}_\mathfrak{k}) \hat{u}_{H,\mathfrak{k}}^{(l+j)} \right\|_{\mathcal{A}}. \end{aligned}$$

We already have estimates for all the terms above except the second. This can be easily found by applying Lemma 3.1 with  $M1$  given by the OLOD and  $M2$  by the MLOD solving (12) and (9) respectively. Then, with  $a_1 = \hat{a}_\mathfrak{k}, a_2 = \tilde{a}_\mathfrak{k}, m_1 = \hat{m}_\mathfrak{k} = \tilde{m}_\mathfrak{k} = m_2, T_H^1 = \hat{T}_H^\mathfrak{k}$  and  $T_H^2 = \tilde{T}_H^\mathfrak{k}$  together with (13) yields

$$\left\| \tilde{T}_H^\mathfrak{k} f^{(l+j)} - \hat{T}_H^\mathfrak{k} f^{(l+j)} \right\|_{\mathcal{A}} \lesssim \left( \max_{T \in \mathcal{T}_H} E_T \right) \mathfrak{k}^{d/2} \left\| \hat{T}_H^\mathfrak{k} f^{(l+j)} \right\|_{\mathcal{A}}.$$

Due to the coercivity condition in (15) together with (26) and the interpolation property, we can derive a constant upper bound for  $\left\| \hat{u}_{H,\mathfrak{k}}^{(l+j)} \right\|_{\mathcal{A}}$ . Hence, similar arguments used for (25) yield

$$\left\| \tilde{u}_{H,\mathfrak{k}}^{(l+j)} - \hat{u}_{H,\mathfrak{k}}^{(l+j)} \right\|_{\mathcal{A}} \lesssim \left( \max_{T \in \mathcal{T}_H} E_T \right) \mathfrak{k}^{d/2}. \quad (28)$$

Theorem 4.5, (14) of Theorem 2.5 and (28) imply that

$$\left\| u^{(l+j)} - \hat{u}_{H,\mathfrak{k}}^{(l+j),ms} \right\|_{\mathcal{A}} \lesssim H^2 + g(\mathfrak{k}) + 2 \left( \max_{T \in \mathcal{T}_H} E_T \right) \mathfrak{k}^{d/2} + \left( \max_{T \in \mathcal{T}_H} E_T \right) \mathfrak{k}^{d/2}. \quad \square$$

**Theorem 4.9** (Eigenvalue estimate). *Suppose  $\lambda^{(l)}$  and  $\hat{\lambda}_{H,\mathfrak{k}}^{(l)}$  are the  $l$ -th eigenvalues of (2) and (12) respectively with a multiplicity  $r$ . Consider the same setting as in Theorem 4.8 where  $\left\| \hat{u}_{H,\mathfrak{k}}^{(l+j),ms} \right\|_{L^2(\Omega)} = 1$  for each  $j = 0, \dots, r-1$ . Then,*

$$\left| \frac{\hat{\lambda}_{H,\mathfrak{k}}^{(l)} - \lambda^{(l)}}{\lambda^{(l)}} \right| \lesssim H^2 + g(\mathfrak{k}) + \left( \max_{T \in \mathcal{T}_H} E_T \right) \mathfrak{k}^{d/2} + \left( \max_{T \in \mathcal{T}_H} E_T \right)^2 \mathfrak{k}^d.$$

*Proof.* Note that  $\frac{\hat{a}_\mathfrak{k}(\hat{u}_{H,\mathfrak{k}}^{(l)}, \hat{u}_{H,\mathfrak{k}}^{(l)})}{\hat{m}_\mathfrak{k}(\hat{u}_{H,\mathfrak{k}}^{(l)}, \hat{u}_{H,\mathfrak{k}}^{(l)})} = \hat{\lambda}_{H,\mathfrak{k}}^{(l)}$ . Then, we obtain that

$$\begin{aligned} \hat{\lambda}_{H,\mathfrak{k}}^{(l)} - \lambda^{(l)} &= \frac{\hat{a}_\mathfrak{k}(\hat{u}_{H,\mathfrak{k}}^{(l+j)}, \hat{u}_{H,\mathfrak{k}}^{(l+j)})}{\hat{m}_\mathfrak{k}(\hat{u}_{H,\mathfrak{k}}^{(l+j)}, \hat{u}_{H,\mathfrak{k}}^{(l+j)})} - \lambda^{(l)} \\ &\leq \hat{a}_\mathfrak{k}(\hat{u}_{H,\mathfrak{k}}^{(l+j)}, \hat{u}_{H,\mathfrak{k}}^{(l+j)}) - \lambda^{(l)} + \frac{\hat{a}_\mathfrak{k}(\hat{u}_{H,\mathfrak{k}}^{(l+j)}, \hat{u}_{H,\mathfrak{k}}^{(l+j)})}{\hat{m}_\mathfrak{k}(\hat{u}_{H,\mathfrak{k}}^{(l+j)}, \hat{u}_{H,\mathfrak{k}}^{(l+j)})} - \hat{a}_\mathfrak{k}(\hat{u}_{H,\mathfrak{k}}^{(l+j)}, \hat{u}_{H,\mathfrak{k}}^{(l+j)}) \\ &= (\hat{a}_\mathfrak{k} - \tilde{a}_\mathfrak{k})(\hat{u}_{H,\mathfrak{k}}^{(l+j)}, \hat{u}_{H,\mathfrak{k}}^{(l+j)}) + [\tilde{a}_\mathfrak{k}(\hat{u}_{H,\mathfrak{k}}^{(l+j)}, \hat{u}_{H,\mathfrak{k}}^{(l+j)}) - \lambda^{(l)}] + \hat{\lambda}_{H,\mathfrak{k}}^{(l)} \left( \left\| \hat{u}_{H,\mathfrak{k}}^{(l+j),ms} \right\|_{L^2(\Omega)}^2 - \hat{m}_\mathfrak{k}(\hat{u}_{H,\mathfrak{k}}^{(l+j)}, \hat{u}_{H,\mathfrak{k}}^{(l+j)}) \right) \\ &\leq \left| (\hat{a}_\mathfrak{k} - \tilde{a}_\mathfrak{k})(\hat{u}_{H,\mathfrak{k}}^{(l+j)}, \hat{u}_{H,\mathfrak{k}}^{(l+j)}) \right| + \left| \tilde{a}_\mathfrak{k}(\hat{u}_{H,\mathfrak{k}}^{(l+j)}, \hat{u}_{H,\mathfrak{k}}^{(l+j)}) - \lambda^{(l)} \right| + \left| \hat{C}_\lambda \lambda^{(l)} \right| \left| \left\| \hat{u}_{H,\mathfrak{k}}^{(l+j),ms} \right\|_{L^2(\Omega)}^2 - \hat{m}_\mathfrak{k}(\hat{u}_{H,\mathfrak{k}}^{(l+j)}, \hat{u}_{H,\mathfrak{k}}^{(l+j)}) \right|. \end{aligned} \quad (29)$$

We use Theorem 2.2, (14) of Theorem 2.5 and the stability of  $\mathcal{C}$  in the energy norm together with the triangle inequality to estimate the last term as

$$\begin{aligned} &\left\| \hat{u}_{H,\mathfrak{k}}^{(l+j),ms} \right\|_{L^2(\Omega)}^2 - \hat{m}_\mathfrak{k}(\hat{u}_{H,\mathfrak{k}}^{(l+j)}, \hat{u}_{H,\mathfrak{k}}^{(l+j)}) \\ &= m((1 - \hat{\mathcal{C}}_\mathfrak{k})\hat{u}_{H,\mathfrak{k}}^{(l+j)}, (1 - \hat{\mathcal{C}}_\mathfrak{k})\hat{u}_{H,\mathfrak{k}}^{(l+j)}) - m(\hat{u}_{H,\mathfrak{k}}^{(l+j)}, \hat{u}_{H,\mathfrak{k}}^{(l+j)}) \\ &\leq \left| m(\hat{\mathcal{C}}_\mathfrak{k}\hat{u}_{H,\mathfrak{k}}^{(l+j)}, \hat{\mathcal{C}}_\mathfrak{k}\hat{u}_{H,\mathfrak{k}}^{(l+j)}) \right| + \left| m(\hat{u}_{H,\mathfrak{k}}^{(l+j)}, \hat{\mathcal{C}}_\mathfrak{k}\hat{u}_{H,\mathfrak{k}}^{(l+j)}) \right| + \left| m(\hat{\mathcal{C}}_\mathfrak{k}\hat{u}_{H,\mathfrak{k}}^{(l+j)}, \hat{u}_{H,\mathfrak{k}}^{(l+j)}) \right| \\ &\lesssim \left( \left\| \hat{\mathcal{C}}_\mathfrak{k}\hat{u}_{H,\mathfrak{k}}^{(l+j)} \right\|_{\mathcal{A}}^2 + 2 \left\| \hat{\mathcal{C}}_\mathfrak{k}\hat{u}_{H,\mathfrak{k}}^{(l+j)} \right\|_{\mathcal{A}} \left\| \hat{u}_{H,\mathfrak{k}}^{(l+j)} \right\|_{\mathcal{A}} \right) H^2 \\ &\lesssim \left( \left\| (\mathcal{C} - \mathcal{C}_\mathfrak{k})\hat{u}_{H,\mathfrak{k}}^{(l+j)} \right\|_{\mathcal{A}}^2 + \left\| (\mathcal{C}_\mathfrak{k} - \hat{\mathcal{C}}_\mathfrak{k})\hat{u}_{H,\mathfrak{k}}^{(l+j)} \right\|_{\mathcal{A}}^2 + 2 \left\| (\mathcal{C} - \mathcal{C}_\mathfrak{k})\hat{u}_{H,\mathfrak{k}}^{(l+j)} \right\|_{\mathcal{A}} \left\| \hat{u}_{H,\mathfrak{k}}^{(l+j)} \right\|_{\mathcal{A}} \right. \\ &\quad \left. + \left\| (\mathcal{C}_\mathfrak{k} - \hat{\mathcal{C}}_\mathfrak{k})\hat{u}_{H,\mathfrak{k}}^{(l+j)} \right\|_{\mathcal{A}} \left\| \hat{u}_{H,\mathfrak{k}}^{(l+j)} \right\|_{\mathcal{A}} + 3 \left\| \hat{u}_{H,\mathfrak{k}}^{(l+j)} \right\|_{\mathcal{A}}^2 \right) H^2 \\ &\lesssim \left\| \hat{u}_{H,\mathfrak{k}}^{(l+j)} \right\|_{\mathcal{A}}^2 \left( g^2(\mathfrak{k}) + 2g(\mathfrak{k}) + 3 + \left( \max_{T \in \mathcal{T}_H} E_T \right)^2 \mathfrak{k}^d + \left( \max_{T \in \mathcal{T}_H} E_T \right) \mathfrak{k}^{d/2} \right) H^2. \end{aligned} \quad (31)$$

Next, let us find an estimate for the middle term in (29). Recall that by definition, it holds that

$$\tilde{a}_{\mathfrak{k}}(\hat{u}_{H,\mathfrak{k}}^{(l+j)}, \hat{u}_{H,\mathfrak{k}}^{(l+j)}) - \lambda^{(l)} = a((1 - \mathcal{C}_{\mathfrak{k}})\hat{u}_{H,\mathfrak{k}}^{(l+j)}, \hat{u}_{H,\mathfrak{k}}^{(l+j)}) - \lambda^{(l)}.$$

Since  $(1 - \mathcal{C}_{\mathfrak{k}})\hat{u}_{H,\mathfrak{k}}^{(l+j)} \in V_{H,\mathfrak{k}}^{ms}$ , by the construction in (24), we obtain that

$$\begin{aligned} a((1 - \mathcal{C}_{\mathfrak{k}})\hat{u}_{H,\mathfrak{k}}^{(l+j)}, \hat{u}_{H,\mathfrak{k}}^{(l+j)}) &\leq \left\| (1 - \mathcal{C}_{\mathfrak{k}})\hat{u}_{H,\mathfrak{k}}^{(l+j)} \right\|_{\mathcal{A}}^2 + \left\| (\mathcal{C} - \mathcal{C}_{\mathfrak{k}})\hat{u}_{H,\mathfrak{k}}^{(l+j)} \right\|_{\mathcal{A}} \left\| \hat{u}_{H,\mathfrak{k}}^{(l+j)} \right\|_{\mathcal{A}} \\ &\leq \left\| (1 - \widehat{\mathcal{C}}_{\mathfrak{k}})\hat{u}_{H,\mathfrak{k}}^{(l+j)} \right\|_{\mathcal{A}}^2 + \left\| (\mathcal{C}_{\mathfrak{k}} - \widehat{\mathcal{C}}_{\mathfrak{k}})\hat{u}_{H,\mathfrak{k}}^{(l+j)} \right\|_{\mathcal{A}}^2 + \left\| (\mathcal{C} - \mathcal{C}_{\mathfrak{k}})\hat{u}_{H,\mathfrak{k}}^{(l+j)} \right\|_{\mathcal{A}} \left\| \hat{u}_{H,\mathfrak{k}}^{(l+j)} \right\|_{\mathcal{A}}. \end{aligned}$$

Combining with (23), we arrive at

$$\begin{aligned} \tilde{a}_{\mathfrak{k}}(\hat{u}_{H,\mathfrak{k}}^{(l+j)}, \hat{u}_{H,\mathfrak{k}}^{(l+j)}) - \lambda^{(l)} &\leq \left\| u^{(l+j)} - \hat{u}_{H,\mathfrak{k}}^{(l+j),ms} \right\|_{\mathcal{A}}^2 - \lambda^{(l)} \left\| u^{(l+j)} - \hat{u}_{H,\mathfrak{k}}^{(l+j),ms} \right\|_{L^2(\Omega)}^2 \\ &\quad + \left\| (\mathcal{C}_{\mathfrak{k}} - \widehat{\mathcal{C}}_{\mathfrak{k}})\hat{u}_{H,\mathfrak{k}}^{(l+j)} \right\|_{\mathcal{A}}^2 + \left\| (\mathcal{C} - \mathcal{C}_{\mathfrak{k}})\hat{u}_{H,\mathfrak{k}}^{(l+j)} \right\|_{\mathcal{A}} \left\| \hat{u}_{H,\mathfrak{k}}^{(l+j)} \right\|_{\mathcal{A}} \\ &\lesssim \left\| u^{(l+j)} - \hat{u}_{H,\mathfrak{k}}^{(l+j),ms} \right\|_{\mathcal{A}}^2 + \left\| (\mathcal{C}_{\mathfrak{k}} - \widehat{\mathcal{C}}_{\mathfrak{k}})\hat{u}_{H,\mathfrak{k}}^{(l+j)} \right\|_{\mathcal{A}}^2 + \left\| (\mathcal{C} - \mathcal{C}_{\mathfrak{k}})\hat{u}_{H,\mathfrak{k}}^{(l+j)} \right\|_{\mathcal{A}} \left\| \hat{u}_{H,\mathfrak{k}}^{(l+j)} \right\|_{\mathcal{A}}. \end{aligned} \quad (32)$$

The above inequality can be easily estimated using Theorems 4.8, 2.2 and (14) of Theorem 2.5.

Using (13), and substituting (30) and (32) in (29), we find the desired estimate as

$$\begin{aligned} \left| \frac{\hat{\lambda}_{H,\mathfrak{k}}^{(l)} - \lambda^{(l)}}{\lambda^{(l)}} \right| &\lesssim \left( \max_{T \in \mathcal{T}_H} E_T \right) \mathfrak{k}^{d/2} \left\| \hat{u}_{H,\mathfrak{k}}^{(l+j)} \right\|_{\mathcal{A}}^2 + \left( H^2 + g(\mathfrak{k}) + \left( \max_{T \in \mathcal{T}_H} E_T \right) \mathfrak{k}^{d/2} \right)^2 + \left( \max_{T \in \mathcal{T}_H} E_T \right)^2 \mathfrak{k}^d \left\| \hat{u}_{H,\mathfrak{k}}^{(l+j)} \right\|_{\mathcal{A}}^2 \\ &\quad + g(\mathfrak{k}) \left\| \hat{u}_{H,\mathfrak{k}}^{(l+j)} \right\|_{\mathcal{A}}^2 + \left( 3 + g(\mathfrak{k}) + \left( \max_{T \in \mathcal{T}_H} E_T \right) \mathfrak{k}^{d/2} \right) H^2 \left\| \hat{u}_{H,\mathfrak{k}}^{(l+j)} \right\|_{\mathcal{A}}^2 \\ &\lesssim \left( H^2 + g(\mathfrak{k}) + \left( \max_{T \in \mathcal{T}_H} E_T \right) \mathfrak{k}^{d/2} + \left( \max_{T \in \mathcal{T}_H} E_T \right)^2 \mathfrak{k}^d \right) \left\| \hat{u}_{H,\mathfrak{k}}^{(l+j)} \right\|_{\mathcal{A}}^2. \end{aligned}$$

The result follows, since  $\left\| \hat{u}_{H,\mathfrak{k}}^{(l+j)} \right\|_{\mathcal{A}}^2$ , similar to (26), can be bounded above by a constant due to  $\widehat{a}(\cdot, \cdot)$ -coercivity.  $\square$

## 5 Numerical experiments

In this section, we illustrate our theoretical developments with several numerical experiments. We focus on the OLOD method and its alternate variant with the  $s$ -values from Section 2.5. For details in the calculation of  $E_T$  (if desired for error control) and discussions of the run-time complexity, we refer to [MV22, Section 5]. Note that aspects on the implementation of the LOD (without offline-online strategy) are explained in [EHMP19]. Our code is based on [HK19] and [Ver21], and freely available at [Kol24].

**Remark 5.1.** In our numerical experiments, we will focus on the approximation of the lowest non-trivial eigenvalue, but emphasize that the theory of Section 4 is also valid for multiple and/or higher eigenvalues. By our focus on the lowest eigenvalue, we circumvent any possible numerical challenges well-known for high eigenvalues such as spectral pollution [LABV90, LS10]. Furthermore, it is known that (higher) eigenvalues may “cross” in its dependence on the random parameter, leading to difficulties in the correct identification and “matching” of corresponding eigenvalues and eigenfunctions [Kat95]. We emphasize that our method and error estimates is targeted at accurate and efficient approximations for single realizations/samples and we do not consider the possibility of crossing eigenvalues in our numerically experiments either.

### 5.1 Experiments for the OLOD method

We consider  $\Omega = [0, 1]^d$  for  $d = 1, 2$ . The spectral bounds are taken to be  $\alpha = 0.1$  and  $\beta = 1$ . We consider  $\mathfrak{k} = 3$  for the LOD formulation and use the standard finite element method on a fine mesh as our reference solver. We measure the root mean square error (RMSE) between the reference eigenvalue and the OLOD eigenvalues against various probabilities  $p$  and the coarse mesh size  $H$  over  $N = 200$  samples.

**Remark 5.2.** The elliptic eigenvalue problem may produce multiple eigenvalues. For reasons of comparison, we consider an averaged eigenvalue of the two smallest non-trivial eigenvalues in our experiment.



### 5.1.1 One-dimensional experiments

In the one-dimensional case, we use a fixed value of  $\varepsilon = 2^{-7}$  where we randomly assign the value 0.1 to each interval of length  $\varepsilon$ . The fine mesh size is taken to be  $h = 2^{-8}$ . Figure 3 shows the error convergence with respect to  $H$  (left) and the defect probability  $p$  (right). In Figure 3a, we observe a second order convergence, which confirms our theoretical findings in Theorem 4.9. For finer  $H$ , we see that the convergence becomes slower the larger  $p$  is. This is most probably due to the consistency error in the offline-online strategy, which is expected to grow with  $p$  and to dominate LOD spatial discretization error for sufficiently fine meshes. Similar  $H$ -convergence rates can also be observed in the two-dimensional experiments (data not shown). Having confirmed the expected  $H$ -convergence, we completely focus on the error dependence on  $p$  in the following and choose rather small values of  $H$  to concentrate on the consistency error.

Figure 3b illustrates the RMSE against probability  $p$  for various  $H$  sizes. We notice a less than 2% RMSE up to 10% of defect probability. We further observe that on each  $H$ , the corresponding error is almost constant for probabilities smaller than 5%. Thereafter the error is only slightly growing.

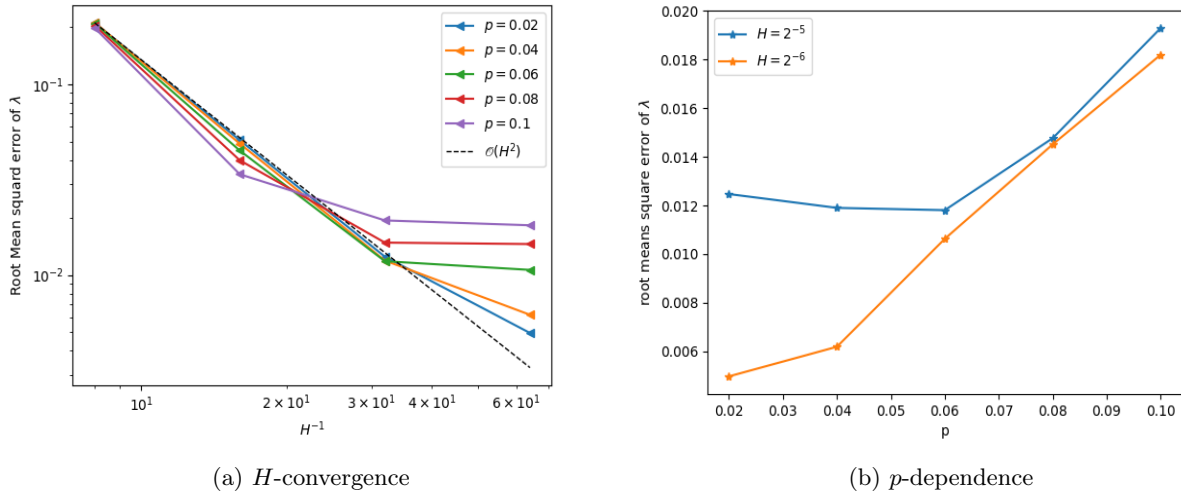


Figure 3: The one-dimensional random checkerboard for  $\varepsilon = 2^{-7}$  with a sample size 200.

### 5.1.2 Two-dimensional experiments

Figure 4 illustrates two-dimensional results for the random checkerboard (left) and random erasure (right) shown in Figure 1 in Section 1. The parameters are set to  $d = 2$ ,  $\varepsilon = 2^{-7}$  and  $h = 2^{-8}$ .

Again, our OLOD method shows a very promising performance with a RMSE of a few percent for reasonable defect probabilities. For instance, the random checkerboard in Figure 4a shows RMSEs less than 10% for  $H = 2^{-6}$  and a defect probability up to 10%. In the random erasure, Figure 4b, RMSEs are even lower, more precisely for  $H = 2^{-6}$ , we observe less than 2% error for material defects up to 10%.

## 5.2 Experiments with the alternate offline-online strategy

In this section, we compare the accuracy of the OLOD and its alternate offline-online strategy (from Section 2.5) for the random checkerboard. The one- and two-dimensional comparisons are depicted in the Figures 5 and 6, respectively. The domain, spectral bounds and the LOD parameters are the same as in Section 5.1. We only compare the results for the smaller mesh sizes  $H = 2^{-5}$  and  $H = 2^{-6}$  to focus on the consistency error and reduce the influence of any discretization errors. In both dimensions the alternate method produces improved results for larger  $p$  as expected. Particularly in two dimensions, we can observe an RMSE less than  $\sim 6\%$  for about 10% of material defects. For the one-dimensional case, as expected both methods produce better results with an RMSE of  $\sim 4\%$  at a 10% material error. However, for much smaller probabilities of material error in the 1D case, slightly better results can be noticed for the OLOD with sum constraint one. We emphasize that this is no contradiction of our theoretical derivations as we only considered limits  $\varepsilon \rightarrow 0$  there. As expected from the choice of  $s$ , the difference between the

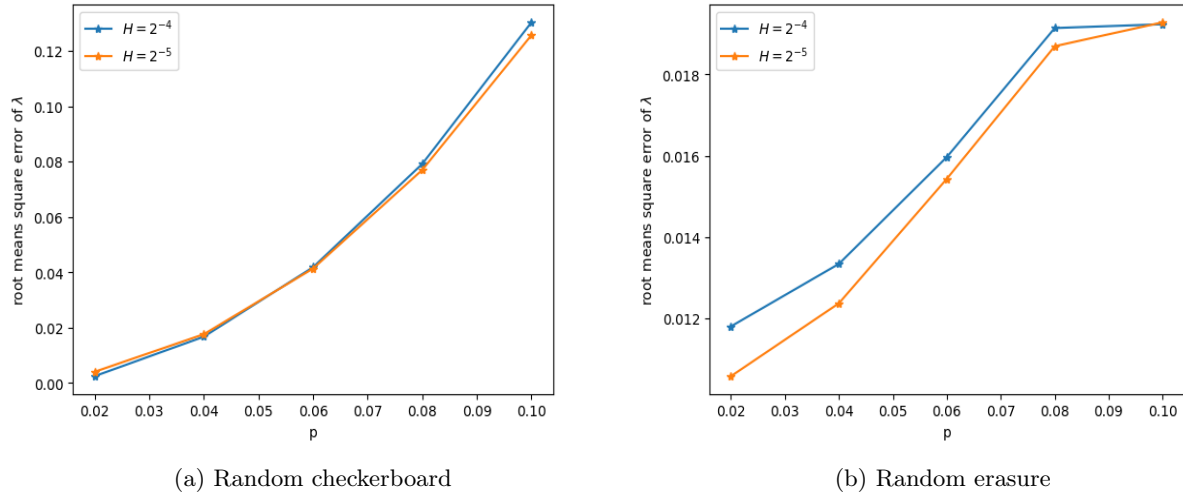


Figure 4: The two-dimensional random checkerboard for  $\varepsilon = 2^{-7}$  with a sample size 200.

sum constraint one model and the alternate variant becomes more prominent with growing  $p$ . We emphasize that, although our derivations were based on one-dimensional heuristics, the two-dimensional results are very promising and underline the potential of our approach.

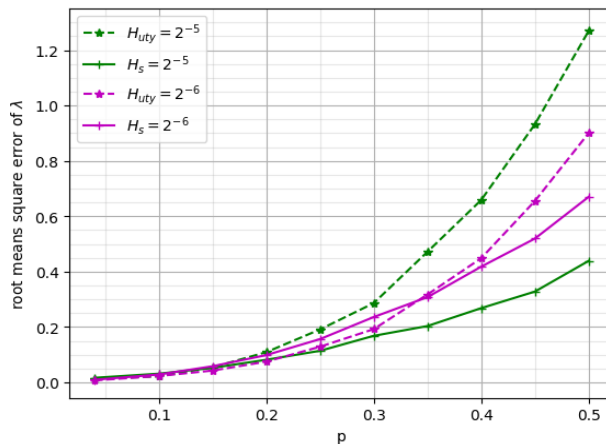


Figure 5: Comparison of offline-online strategy with sum constraint one and alternate version in one-dimension for  $\varepsilon = 2^{-7}$  over 200 samples.

## 6 Conclusion

We outlined a practically feasible approach of the Localized Orthogonal Decomposition (LOD) based offline-online strategy for the elliptic eigenvalue problem with randomly perturbed coefficients suited for Monte-Carlo-type simulations. We analyzed the errors in eigenvalue and eigenfunction approximation for any given realization of the coefficient. We further introduced a heuristic offline-online strategy that is uniquely adaptable to the defect distribution by exploiting the stochastic aspects of the problem. Our numerical experiments illustrate the good performance of our strategy, especially they indicate the superiority of the alternate method adapting the sum constraint. Since our derivation were based on rather simple one-dimensional heuristics, it might be interesting to investigate more sophisticated “optimisation” strategies as well as the application to other probability distributions in

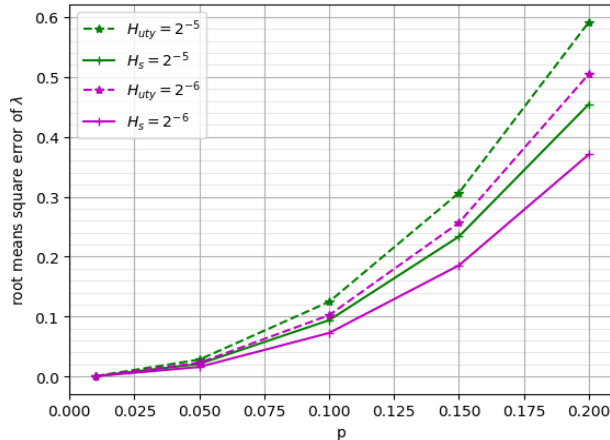


Figure 6: Comparison of offline-online strategy with sum constraint one and alternate version in two-dimension for  $\varepsilon = 2^{-7}$  over 200 samples.

future research. Moreover, the periodicity assumption on the domain clearly plays a major role in this paper, which we hope to reduce in future research.

## Acknowledgments

This research is funded by the Deutsche Forschungsgemeinschaft (DFG, German Research Foundation) under project number 496556642. BV additionally acknowledges support by the Deutsche Forschungsgemeinschaft (DFG, German Research Foundation) under Germany's Excellence Strategy – EXC-2047/1 – 390685813.

## References

- [ABS13] Assyr Abdulle, Andrea Barth, and Christoph Schwab. Multilevel Monte Carlo methods for stochastic elliptic multiscale PDEs. *Multiscale Model. Simul.*, 11(4):1033–1070, 2013.
- [ALB11] A. Anantharaman and C. Le Bris. A numerical approach related to defect-type theories for some weakly random problems in homogenization. *Multiscale Model. Simul.*, 9(2):513–544, 2011.
- [ALB12] A. Anantharaman and C. Le Bris. Elements of mathematical foundations for numerical approaches for weakly random homogenization problems. *Commun. Comput. Phys.*, 11(4):1103–1143, 2012.
- [AP19] R. Altmann and D. Peterseim. Localized computation of eigenstates of random Schrödinger operators. *SIAM J. Sci. Comput.*, 41(6):B1211–B1227, 2019.
- [BH17] Donald L. Brown and Viet Ha Hoang. A hierarchical finite element Monte Carlo method for stochastic two-scale elliptic equations. *J. Comput. Appl. Math.*, 323:16–35, 2017.
- [BNT07] Ivo Babuška, Fabio Nobile, and Raúl Tempone. A stochastic collocation method for elliptic partial differential equations with random input data. *SIAM J. Numer. Anal.*, 45(3):1005–1034, 2007.
- [BO89] I. Babuška and J. E. Osborn. Finite element-Galerkin approximation of the eigenvalues and eigenvectors of selfadjoint problems. *Math. Comp.*, 52(186):275–297, 1989.
- [BO90] Uday Banerjee and John E. Osborn. Estimation of the effect of numerical integration in finite element eigenvalue approximation. *Numer. Math.*, 56(8):735–762, 1990.
- [BO91] I. Babuška and J. Osborn. Eigenvalue problems. In *Handbook of numerical analysis, Vol. II*, Handb. Numer. Anal., II, pages 641–787. North-Holland, Amsterdam, 1991.
- [BSZ11] Andrea Barth, Christoph Schwab, and Nathaniel Zollinger. Multi-level Monte Carlo finite element method for elliptic PDEs with stochastic coefficients. *Numer. Math.*, 119(1):123–161, 2011.

- [BTZ04] Ivo Babuška, Raúl Tempone, and Georgios E. Zouraris. Galerkin finite element approximations of stochastic elliptic partial differential equations. *SIAM J. Numer. Anal.*, 42(2):800–825, 2004.
- [CGST11] K. A. Cliffe, M. B. Giles, R. Scheichl, and A. L. Teckentrup. Multilevel Monte Carlo methods and applications to elliptic PDEs with random coefficients. *Comput. Vis. Sci.*, 14(1):3–15, 2011.
- [CL02] P. G. Ciarlet and J. L. Lions, editors. *Handbook of numerical analysis. Vol. VIII*. Handbook of Numerical Analysis, VIII. North-Holland, Amsterdam, 2002. Solution of equations in  $\mathbb{R}^n$ . Part 4, Techniques of scientific computing. Part 4, Numerical methods for fluids. Part 2.
- [DBO01] Manas K. Deb, Ivo M. Babuška, and J. Tinsley Oden. Solution of stochastic partial differential equations using Galerkin finite element techniques. *Comput. Methods Appl. Mech. Engrg.*, 190(48):6359–6372, 2001.
- [EGH15] Daniel Elfverson, Victor Ginting, and Patrick Henning. On multiscale methods in Petrov-Galerkin formulation. *Numer. Math.*, 131(4):643–682, 2015.
- [EHMP19] Christian Engwer, Patrick Henning, Axel Målqvist, and Daniel Peterseim. Efficient implementation of the localized orthogonal decomposition method. *Comput. Methods Appl. Mech. Engrg.*, 350:123–153, 2019.
- [EKM24] Mehdi Elasmî, Felix Krumbiegel, and Roland Maier. Neural numerical homogenization based on deep ritz corrections. arXiv preprint 2411.14084, 2024.
- [Eva10] Lawrence C. Evans. *Partial differential equations*, volume 19 of *Graduate Studies in Mathematics*. American Mathematical Society, Providence, RI, second edition, 2010.
- [GWZ14] Max D. Gunzburger, Clayton G. Webster, and Guannan Zhang. Stochastic finite element methods for partial differential equations with random input data. *Acta Numer.*, 23:521–650, 2014.
- [HK19] Fredrik Hellman and Tim Keil. Gridlod. GitHub repository, <https://github.com/fredrikhellman/gridlod>, 2019.
- [HM14] Patrick Henning and Axel Målqvist. Localized orthogonal decomposition techniques for boundary value problems. *SIAM J. Sci. Comput.*, 36(4):A1609–A1634, 2014.
- [Kat95] Tosio Kato. *Perturbation theory for linear operators*. Classics in Mathematics. Springer-Verlag, Berlin, 1995. Reprint of the 1980 edition.
- [Kol24] Dilini Kolombage. random-perturbations-evp: preprint version. software, <https://doi.org/10.5281/zenodo.14237300>, 2024.
- [KSS12] Frances Y. Kuo, Christoph Schwab, and Ian H. Sloan. Quasi-Monte Carlo finite element methods for a class of elliptic partial differential equations with random coefficients. *SIAM J. Numer. Anal.*, 50(6):3351–3374, 2012.
- [LABV90] X. Llobet, K. Appert, A. Bondeson, and J. Vaclavik. On spectral pollution. *Comput. Phys. Comm.*, 59(2):199–216, 1990.
- [LBLT14] Claude Le Bris, Frédéric Legoll, and Florian Thomines. Multiscale finite element approach for “weakly” random problems and related issues. *ESAIM Math. Model. Numer. Anal.*, 48(3):815–858, 2014.
- [LS10] Mathieu Lewin and Éric Séré. Spectral pollution and how to avoid it (with applications to Dirac and periodic Schrödinger operators). *Proc. Lond. Math. Soc. (3)*, 100(3):864–900, 2010.
- [MP14] Axel Målqvist and Daniel Peterseim. Localization of elliptic multiscale problems. *Math. Comp.*, 83(290):2583–2603, 2014.
- [MP15] Axel Målqvist and Daniel Peterseim. Computation of eigenvalues by numerical upscaling. *Numer. Math.*, 130(2):337–361, 2015.
- [MP21] A. Målqvist and D. Peterseim. *Numerical homogenization by localized orthogonal decomposition*, volume 5 of *SIAM Spotlights*. Society for Industrial and Applied Mathematics (SIAM), Philadelphia, PA, [2021] ©2021.
- [MV22] Axel Målqvist and Barbara Verfürth. An offline-online strategy for multiscale problems with random defects. *ESAIM Math. Model. Numer. Anal.*, 56(1):237–260, 2022.
- [Owh17] Houman Owhadi. Multigrid with rough coefficients and multiresolution operator decomposition from hierarchical information games. *SIAM Rev.*, 59(1):99–149, 2017.
- [SF73] Gilbert Strang and George J. Fix. *An analysis of the finite element method*. Prentice-Hall Series in Automatic Computation. Prentice-Hall, Inc., Englewood Cliffs, NJ, 1973.

- [Ver21] Barbara Verfürth. Gridlod-random-perturbations. GitHub repository, <https://github.com/BarbaraV/gridlod-random-perturbations>, 2021.
- [XZO19] Hehu Xie, Lei Zhang, and Houman Owhadi. Fast eigenpairs computation with operator adapted wavelets and hierarchical subspace correction. *SIAM J. Numer. Anal.*, 57(6):2519–2550, 2019.
- [ZCH15] Zhiwen Zhang, Maolin Ci, and Thomas Y. Hou. A multiscale data-driven stochastic method for elliptic PDEs with random coefficients. *Multiscale Model. Simul.*, 13(1):173–204, 2015.